Comparing Continuous Methane Monitoring Technologies for High-Volume Emissions: A Single-Blind Controlled Release Study

Zhenlin Chen,[†,||] Sahar H. El Abbadi,[‡,||] Evan D. Sherwin,[‡] Philippine M. Burdeau,[¶] Jeffrey S. Rutherford,[§] Yuanlei Chen,[¶] Zhan Zhang,[¶] and Adam R. Brandt[*,¶]

†*Energy Science & Engineering, Stanford University, Stanford, California 94305*

‡*Lawrence Berkeley National Laboratory, Berkeley, California 94720, United States*

¶*Energy Science & Engineering, Stanford University, Stanford, California 94305, United States*

§*Highwood Emissions Management, Calgary, Alberta T2P 2V1, Canada*

||*Denotes equal contribution*

E-mail: abrandt@stanford.edu

Abstract

Methane emissions from oil and gas operations are a primary concern for climate change mitigation. While traditional methane detection relies on periodic surveys that yield episodic data, continuous monitoring solutions promise to offer consistent insights and a richer understanding of emission inventories. Despite this promise, the detection and quantification ability of continuous monitoring solutions remain unclear. To address this uncertainty, our study comprehensively assessed 8 commercial continuous monitoring solutions using controlled release tests to simulate high-volume venting (e.g., uncontrolled tanks, pneumatics, unlit flares), which accounts for a significant fraction of total emissions from oil and gas systems. The performance of each team varied: when comparing reported results on a second-by-second basis, all teams reported false positive rates below 10%. For true positive rates, 4 out of 8 systems exceed 80%. In the field test where continuous monitoring solutions identified and reported an emission event, all systems' reliability of identification surpassed 70%. When systems reported there was no emission event, the reliability of non-emission identification varied from 29.4% to 96.2%. Among 5 systems tested for quantifying the daily average emission rate released by the Stanford team, all underestimated by an average of 74.38% emissions. This indicates that their application in emissions reporting or regulation may be premature. The variability in monitor performance underscores the importance of understanding systems' strengths and limitations before their broader adoption in methane mitigation approaches or regulatory frameworks.

Keywords

Methane, emission mitigation, single-blind, controlled release, emission quantification, venting

Synopsis

Addressing the urgent requirement for precise oil and gas site-level detection and the creation of methane emission inventories for high-volume emissions, this study assesses the capabilities of various continuous monitoring solutions in their role in methane mitigation.

Introduction

Anthropogenic methane (CH_4) significantly influences global warming, with its impact over 20 years being 80 times greater than that of carbon dioxide .[1] Reflecting a heightened legislative focus on mitigating such impacts, the US Inflation Reduction Act (IRA) has instituted penalties for methane emissions from oil and gas companies.[2] While significant advancements have been made in the detection and quantification of methane emissions, challenges persist in achieving consistent and continuous monitoring over time. This is crucial for accurately assessing the expansive and variable nature of emissions from oil and gas infrastructures.[3–5]

Traditional detection methods, including periodic surveys, are valued for their direct measurement, cost-effectiveness, and localized data precision.[6–8] However, these methods have limitations in accurately characterizing methane emissions from facilities with intermittent emission profiles. For example, research on aerial surveys in the Permian Basin by Cusworth et al. in 2019 revealed that large emissions are typically short-lived and sporadic.[9] This sporadic nature poses a challenge: while regional emissions can be detected, significant high-emission events (e.g., uncontrolled tanks, pneumatics, unlit flares) might be overlooked, leading to potential biases and gaps in emission assessments.[10–12] This oversight can adversely affect the development of emission inventories, a critical process mandated by the Environmental Protection Agency (EPA) which requires oil and gas operators to report their emissions to the government for regulatory and environmental monitoring.[13] To mitigate the challenges of monitoring sporadic emissions, repeat sampling is required, which increases the cost of periodic surveys. These challenges have raised interest in continuous monitoring solutions that can capture both intermittent and sustained emissions and account for variability in frequency and duration in real time.[9,14]

A typical continuous monitoring system strategically deploys multiple stationary sensors, often solar-powered, around infrastructure to measure gas concentrations. These systems utilize gas concentration measurements or optical imaging to detect and quantify methane emissions.[15,16] Their capability for extended monitoring allows for real-time detection of methane emissions, aiding oil and gas operators in more accurately reporting facility-level emissions to the government. [17,18] Such immediate access to emission data enables the operators to quickly respond to leaks, thereby reducing emissions and enhancing the accuracy of greenhouse gas emission records. Consequently, this contributes to more efficient leak detection and repair (LDAR) practices in the industry.[19,20]

The development of continuous monitoring solutions is ongoing, and a comprehensive understanding of their full capabilities remains an area of research.[15,21–23] The most recent study in this area was conducted by Bell et al. in 2023.[23] The researchers examined 11 different continuous monitoring technologies, leveraging an expansive dataset produced by the Methane Emissions Technology Evaluation Center (METEC) at Colorado State University. However, METEC tests are limited to emission rates below 6.4 kg CH_4/hr and cannot conduct controlled emissions in the 10s, 100s, and 1000s of kg CH_4/hr that represent the majority of total oil and gas system emissions across various regions.[24]

Addressing the limited range of emission testing, we have designed a setup that can gauge a wider spectrum of methane emissions, ranging from as low as 0.037 to over 1,500 kg CH_4/hr. At this large scale, we can recreate venting conditions observed from large equipment pressure-relief failure, tank control breakdowns, and unlit flares.[25,26]

Furthermore, the Bell et al. study maintains the anonymity of the technologies evaluated due to contractual obligations. This approach, while necessary, makes it more challenging to directly link the results to a particular continuous monitoring system.[23]

We provide a transparent association between results and their respective continuous monitoring systems. Such clarity allows us to align our tailored performance metrics with the specific technologies, enhances the replicability of our research, and aids practical applications by oil and gas operators and regulatory bodies.

We conducted the first independent, high-volume single-blind controlled release test, evaluating 8 identifiable commercial continuous monitoring systems. These systems include point sensor networks from Ecotec, SOOFIE, Project Canary, Qube Technologies, and Sensirion. We also evaluated camera-based technologies from Andium, Kuva systems, and Oiler.[23,27–34] At the core of our study, we developed specialized detection evaluation metrics for continuous monitors, focusing on the sensors' proficiency in emission detection and their precision in quantification. This study highlights the variability in the performance of camera sensors and point sensor networks, revealing a tendency to underestimate larger emissions. These preliminary insights lead to a broader discussion in the quantification section, where we emphasize the need for careful interpretation of monitoring data. Particularly for precision-critical activities like emissions reporting, our analysis suggests that while continuous monitoring systems are essential for detecting significant emission sources, their use in nuanced applications, such as developing emissions inventories, may require further refinement and validation.

Methods

Experimental overview

We evaluated the methane detection capabilities of continuous monitoring systems from October 10 to December 1, 2022, in Casa Grande, Arizona (USA). This assessment ran concurrently with evaluations of airplanes[35] and satellites.[36] The Stanford University team controlled and metered the gas release rates, while the continuous monitoring systems were set to detect the emissions rate in a single-blind study format. Continuous monitoring companies were not informed about release timings, such as the start and stop points, or the specific mass emission rates. However, they were provided with the coordinates of the gas release equipment [32.8218489°, -111.7857599°] and details of two stack heights. Equipment installation began on October 5, 2022. Technicians from the monitoring companies were not allowed to place equipment within restricted areas (the safety perimeter marked in orange in figure 1) or outside of designated zones (enclosed by a fence visible in figure 1). These technicians were allowed routine supervised site visits to check equipment functionality and make necessary adjustments. Any such visits and changes to the equipment setup are detailed in Supplementary Information (SI) 1.1.

Methane controlled releases

The methane-controlled release experiment was conducted in a desert environment, chosen to simulate optimal conditions for testing continuous monitoring systems and minimizing external influences. This location was intentionally selected to be isolated from other methane sources, aiming so that any methane detected was exclusively from the controlled releases.

Detailed descriptions of the experimental setup, equipment, and methane flow rate data logging are included in El Abbadi et al.[35] and summarized here. Figure 1 depicts the experimental setup, including labels for all continuous monitoring systems.

Briefly, the methane source for all experiments was compressed natural gas (CNG), stored onsite in two trailers provided by Rawhide Leasing and regularly refilled by CNG suppliers in the Phoenix and Tucson area. Initial gas pressure ranged from 3.45 and 17.23 MPa (500-2500 psig), based on trailer fill level. CNG was then transferred to a pressure regulation trailer, where pressure was reduced to 2.76 MPa (400 psig) before being routed to the metering and release setup (illustrated in figure 1). Average methane concentration of CNG was 94.53% (mole percentage of methane), with a standard deviation of 0.62%.

The Stanford field team used the FLIR GasFinder 320 infrared camera to monitor both methane releases and for presence of any ambient methane. In particular, compressed gas trailers and pressure regulation equipment were located within the monitoring perimeter. When Rawhide personnel changed gas supply trailers or modified equipment, the Stanford team documented relevant timestamps and checked for potential leaks with the FLIR camera.

The Stanford field team controlled the gas flow rate from a laptop by adjusting valves in the metering and release trailer. These valves allowed gas to flow through one of three parallel flow paths of different diameters, each fitted with a correspondingly sized Coriolis meter (Emerson MicroMotion) that collected flow measurements at 1Hz. Gas was released from one of two release stacks: 7.3 meters (24 feet) or 3 meters (10 feet) above ground level, referred to as tall and short stacks respectively. The two different heights allow this system to evaluate how continuous monitoring performance changes with releases at different heights, although due to system troubleshooting discussed in El Abbadi et al. rigorous testing of this nature will be the subject of future work.[35] The detailed stack height usage can be found in SI 1.2.

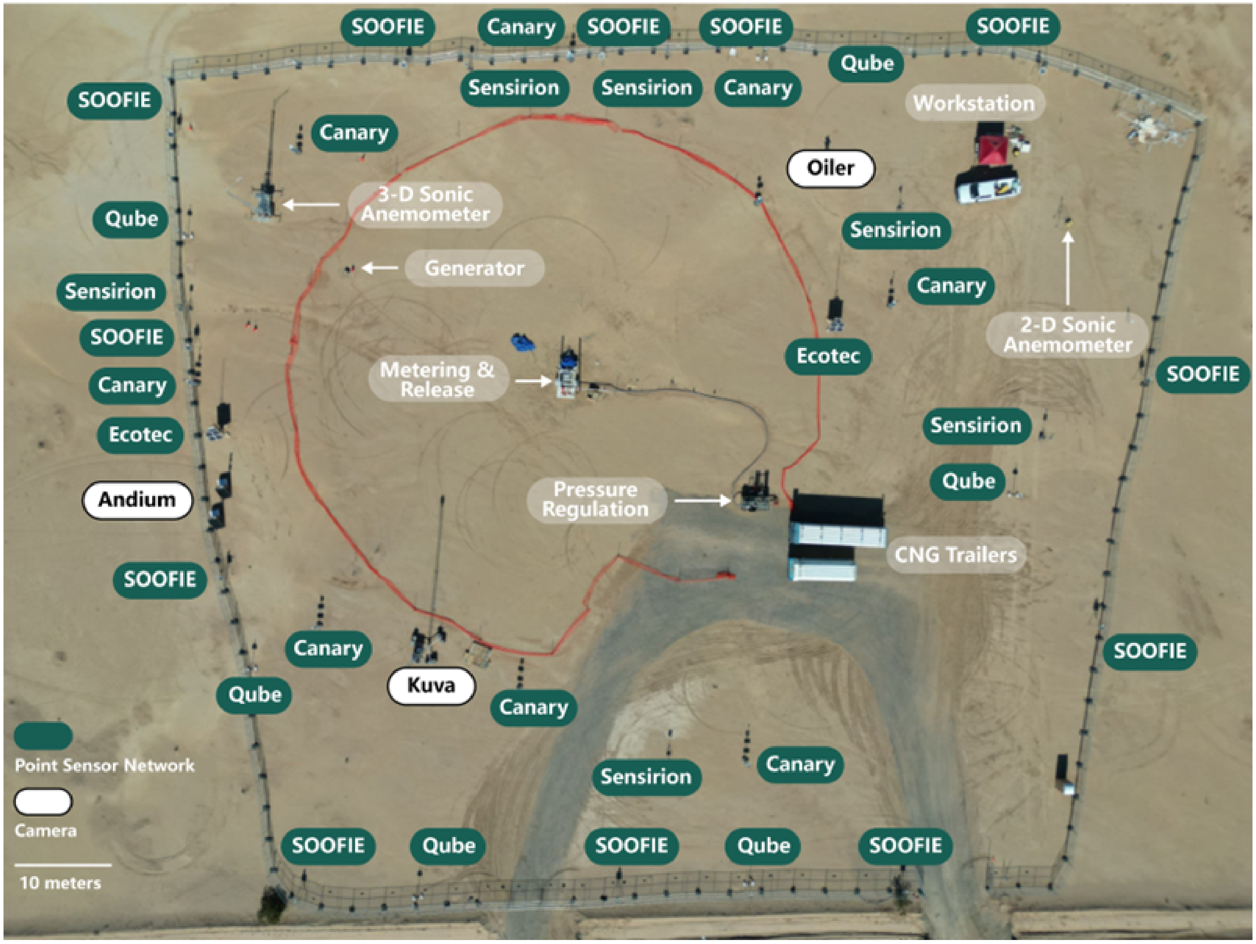

Figure 1: Experimental field site layout. All deployed continuous monitoring units are labeled with the corresponding company name. Methane is supplied from compressed natural gas trailers and is then reduced in pressure at a regulation trailer before it is delivered to the metering and release trailer. Wind data are collected using a 3D sonic anemometer on a 10-meter tower. The Stanford team sets specific flow rates from a workstation. The layout also includes point sensor networks and camera-based technologies positioned at specific locations, with the safety perimeter marked in orange.

The experimental setup closely simulates an unlit flare or tank vent at an oil and gas production site, offering a simpler context compared to the intricate environments of typical facilities. These environments usually feature extensive infrastructure, such as wellheads, tanks, flares, separators, and complex machinery in compressor stations and processing plants, complicating methane detection and quantification. Future research will replicate these intricate conditions to evaluate the performance of monitoring technologies in varied and demanding operational environments.

Safety measures

Trained technicians from Rawhide Leasing managed the natural gas equipment. The Stanford team implemented a 45-meter (150 ft) safety zone around the metering and release area, strictly off-limits during gas release events. Continuous monitoring operators were allowed to access the equipment only during non-release periods. Utilizing a FLIR GasFinder 320 infrared camera, the researchers monitored the dispersal of the gas plume to ensure it remained away from personnel. If any member detected the odor of gas, the Stanford team immediately checked the infrared data and wind conditions to ensure safety at the site.

Descriptions of technologies tested

We evaluated 8 continuous monitoring technologies. Five were point sensor networks which included Ecotec, Project Canary, Qube, Sensirion's Nubo Sphere, and ChampionX's SOOFIE. The remaining three were camera solutions: Andium, Kuva, and Oiler. Table 1 describes the units deployed for this experiment and the official testing dates for each participant. Variations in sample sizes are due to differences in technology deployment, testing periods, and system downtime for maintenance. Detailed records of these variations are available on GitHub, as reported by each team.

Point sensor networks deploy multiple sensors across an area, each detecting methane or hydrocarbons at a particular point in space (X,Y,Z) at high temporal resolution (e.g, 1 Hz). These data, when combined with meteorological information, can be used to pinpoint emission sources. Gas detection techniques used within this category include tunable diode laser absorption spectroscopy (TDLAS), which measures changes in the transmission of light of a frequency that is absorbed by methane, or metal oxide gas sensors (MOS) that detect changes in electrical conductivity when exposed to target gases.[37]

Camera-based technologies adopt infrared imaging systems to capture continuous or intermittent pictures of a test site. Infrared visualization, a predominant method, detects gases by observing light intensity variations due to gas absorption in the infrared spectrum, a passive sensing approach.[16] The imagery, sequenced into videos, is analyzed by continuous monitoring companies along with their collected meteorological data to identify emissions and estimate the emissions rate.[38]

Participants were given the option to evaluate detection performance (reporting binary 0-1 data corresponding to whether gas is emitting), or both detection and quantification performance (reporting the estimated rate of emission in kilograms per hour). It is important to note that the Stanford team did not participate in the analysis of the reports submitted by the teams. Our evaluation of the metrics was exclusively based on the periods that the teams reported their units were and collecting data. This approach aims to represent the actual operational performance of the technologies under review. Andium and Ecotec chose to report solely on detection performance. Hence, their quantification data is marked as "N/A" (not applicable) in Table 1. Kuva initially intended to evaluate both detection and quantification, but their final submission included only detection results. All other participants reported both detection and quantification results. Project Canary requested to limit their evaluation to methane emissions from the short stack. This request was agreed to by the Stanford team before the test.

Continuous monitoring data reporting

The reporting approach we used is modified based on the Advancing Development of Emission Detection (ADED) protocol for continuous monitors.[39,40] Continuous monitoring solutions report emissions events either using a time-averaged emission rate or by reporting an average emission rate for the duration of an emission event. For the time-averaged approach, they typically report a continuous series of release rates averaged over the relevant time in-

Table 1: Participation of different continuous monitoring teams in the experiment

Team name	Technology type	Dates(2022)	Number of units	Time-based event sample (s)[2]	Team-defined event sample[3]	Stanford-defined event sample[4]	Quantification sample[5]
Ecotec	Point sensor network	10/28 – 11/28	2	2,639,159	1,039	185	N/A
Project Canary		10/10 – 11/29	8	1,354,747	37	93	10
Qube		10/10 – 11/23	6	3,147,247	206	232	27
Sensirion		10/10 – 11/30	6	3,738,986	113	253	21
SOOFIE		10/10 – 11/29[1]	12	2,528,490	N/A	N/A	26
Andium	Infrared camera	10/10 – 11/23	2	3,128,980	223	376	N/A
Kuva		10/10 – 11/23	1	914,142	325	321	N/A
Oiler		10/10 – 11/03	1	1,081,843	233	179	13

[1] SOOFIE sensor downtime (11/07 to 11/14): SOOFIE sensors were offline during this period due to a conflict of interest as they are from Scientific Aviation. The company was conducting airplane methane detection tests in Stanford control-release campaign during that time.

[2] Time-based sampling methodology: Samples are recorded every second for a direct comparison between the continuous monitoring reports and the methane releases documented by Stanford. This analysis is specifically conducted during intervals when the technologies are operational. The data is then organized into a confusion matrix to assess the performance of the monitoring systems while they are online.

[3] Team-defined event samples: The table displays events reported by each team, which are then compared against events defined by Stanford. This analysis checks whether sensor-detected emissions corresponds to actual gas releases onsite. Canary's data are limited to short stack height periods following a request from Project Canary before the testing phase. SOOFIE's 15-minute average reporting type is not suitable for event-based detection analysis.

[4] Stanford-defined event samples: The table presents emission events as defined by Stanford. Stanford conducted a wind transport model to define events for point sensor networks, while for camera-based systems, events are defined by the start and end times of emissions.The focus is on correlating these Stanford-defined events with sensor detection to assess if sensors accurately identify gas releases during Stanford's emission events. SOOFIE's 15-minute average reporting time is not suitable for event-based detection analysis.

[5] Quantification sample: Samples of daily average emissions are calculated for each team, with "N/A" indicating non-participation.

terval. When reporting events, the monitors typically report a start and stop time for the emission event, and an average release rate for the entire event. We provided participants with a reporting template for both formats, detailed in SI 1.3. The exact submission date for each team can be found in SI 1.4.

We did not modify or change any participant's reported data. Our study did not assess each team's data processing times in order to maintain data integrity and accurately reflect the sensors' performance under operational conditions. However, we recognize that the speed at which emission data is processed and reported is crucial for the efficacy of continuous monitoring systems. Therefore, we recommend that future research should investigate data processing times to ensure that rapid response capabilities are maintained in practical applications of these technologies.

Data collection and filtering

Gas flow data were collected using three Coriolis gas flow meters, which report whole gas mass flow rates. These data were then converted to methane flow rates, following the methodology presented in El Abbadi et al. 2023.[35]

To ensure the accuracy of our ground truth data, we implemented data filtering practices, including the exclusion of periods during Stanford's internal testing to prevent equipment-related gas releases from skewing results.

To address the influence of variable wind conditions on point sensor network detection accuracy, we developed a wind transport model. This model assessed whether methane from previous releases lingered within twice the radius (or 163.8 meters from the release point) of the field site, using local 10-m wind data. We applied this model for determining start and end times of events for point-sensor networks, but not camera-based systems which directly visualize emission changes, bypassing the need for wind-related adjustments. Detailed explanations of our data collection and filtering methodology are provided in SI 1.5 of our study.

It is important to note that our study did not address whether sensor solutions report the time of expected emission start, based on continuous monitoring solutions' internal dispersion modeling algorithms, or simply the time when their sensors detect an enhancement. While we did not modify the reported data to account for these discrepancies in time measurement and modeling, we recommend that future research investigate the comparison between sensor-reported detection times and those predicted by dispersion models.

Evaluating detection capabilities

We evaluated detection capabilities using two methods: a time-based approach, and an event-based approach. For the event-based approach, we used two methods to classify events: (1) Stanford-defined events and (2) team-reported events. The details of the data processing for detection capability are shown in SI 1.5 and SI 1.6.

Time-based detection

The time-based method offers a straightforward interpretation, representing the least processed data on continuous monitoring performance. It helps answer a simple question: What fraction of the time does a given technology accurately or inaccurately report the state of the emission?

An "Instance" refers to a 1-second interval during which methane emissions are assessed. In our approach, we compared the continuous monitoring reports with the actual methane releases on a second-by-second basis, placing each instance into specific predefined categories (True Positive, True Negative, False Positive, False Negative). For point sensor networks, we account for any time lag between when gas is released and when it arrives at the sensor through a wind transport model. This analysis was strictly performed for periods when the monitoring technologies were reported as operational. Further details of time-based detection can be found in SI 1.7.4.

- **True Positive (TP%)**: the percentage of instances where the system correctly identifies the presence of emissions.
- **False Positive (FP%)**: the percentage of instances where the system incorrectly signals the presence of emissions when there are none.
- **True Negative (TN%)**: the percentage of instances where the system correctly identifies the absence of emissions
- **False Negative (FN%)**: the percentage of instances where the system fails to detect emissions when they are present.

For each technology tested, we determined the total number of sample intervals and classified them as indicated in column 5 of Table 1. The frequency of occurrence for each category within the total number of samples was recorded and expressed as a percentage. These frequencies are thoroughly detailed in figure 3.

Furthermore, we calculate true positive, false positive, true negative, and false negative rates, which are indicative of the monitors' detection capability in finding actual methane emissions on a second-by-second basis. The rates are characterized as follows.

- **True Positive Rate(TPR%)**: Calculated as $\frac{TP}{TP+FN} \times 100$, this is the proportion of non-zero gas release intervals that were accurately detected.
- **False Positive Rate(FPR%)**: Calculated as $\frac{FP}{FP+TN} \times 100$, this is the proportion of intervals that were mistakenly identified as non-zero releases.
- **True Negative Rate(TNR%)**: Calculated as $\frac{TN}{TN+FP} \times 100$, this is the proportion of intervals correctly identified as zero releases.
- **False Negative Rate(FNR%)**: Calculated as $\frac{FN}{FN+TP} \times 100$, this is the proportion of intervals where non-zero releases were incorrectly reported as zero.

We also evaluated the accuracy and precision of the systems, as shown in figure 3. This is crucial for assessing their reliability in detecting emissions.

- **Accuracy**: Calculated as $\frac{TP+TN}{TP+TN+FP+FN} \times 100$, this metric provides a measure of how well the system's measurements agree with the actual state of emissions. It represents the proportion of true positives (TP) and true negatives (TN) out of all samples.
- **Precision**: Calculated as $\frac{TP}{TP+FP} \times 100$, this metric reflects the reliability of the system in reporting emission detection. It represents the proportion of true positive measurements out of the total reported positives, which is the sum of true positives (TP) and false positives (FP).

Event-based detection

We examined results based on "events" or time blocks of continuous emissions or non-emissions. We created two event-based measures that evaluated detection capabilities based on the alignment of Stanford-defined events with team-defined events. The two event-based metrics differ in which kind of event is assumed as the baseline for comparison.

The "Stanford-based event" approach uses Stanford events as the baseline for comparison and determines whether continuous monitors identify gas released during Stanford-released emission events. This is a period in which the Stanford team held a steady emission rate that is more than 1 minute. To assess point sensor networks, we integrated a wind transport model. This model delineates each "Stanford event" by tracking the start of the methane's release and dispersion, defining the end of the event boundaries when the methane has dissipated to twice the experimental area. However, for camera-based technology, we simply measured the duration of gas emission from the start of the release to the end of the release. For an in-depth understanding of how "Stanford events" were determined and the logic behind these approaches, refer to SI 1.5.

For the "team-defined event" approach, we used continuous monitoring solutions' reported time intervals for a given event that they submitted in the data reporting spreadsheet. We determined whether each event has a corresponding and temporally overlapping Stanford gas release.

Note that we do not require a perfect overlap of timing to consider an event covered. We did not want to penalize continuous monitoring solutions for slight misalignment in the start or end times of events. Thus, we use a set of specific overlap criteria for detecting emission and non-emission events, catering to the primary use cases of these continuous monitoring solutions.

When detecting emission events, our primary goal is to ensure that continuous monitors promptly alert oil and gas facility operators. Therefore, if a monitor recognizes an emission during just 10% of the actual emission event's duration (as confirmed by Stanford's measurements), we consider that emission to have been correctly identified. Simply put, even if a continuous monitoring solution only detects a leak for a fraction ($> 10\%$) of its actual occurrence, we deem it a successful detection.

The example of how we adopt the overlap criteria and evaluate the continuous monitoring detection accuracy in different metrics is shown in figure 2. The events reported by the monitors closely align with those defined by Stanford, emphasizing consistency in the metrics. Instances of misalignment, such as false negatives (in orange) and false positives (in red), are recorded in the time-based rules, which are analyzed on a second-by-second basis. However, these instances are not subject to penalties in Stanford-defined and team-defined events-based metrics because of the overlap criteria in place. Gaps in the Stanford-defined events section are due to the exclusion of events lasting less than one minute, or periods when the team reported downtime.

For non-emission periods, minimizing false alarms will ensure efficient allocation of emissions mitigation resources. Hence, we have stricter criteria for false positives in the Stanford-defined event reporting framework. If during a period where no emissions are happening (as confirmed by Stanford), a continuous monitoring solution indicates an emission for more than 10% of that period, we categorize the event as a false positive. This means that to be seen as accurately detecting a non-emission period, the continuous monitoring solutions must correctly identify at least 90% of that period as having no emissions. The specified overlap percentages ensure that the sum of different metrics, when combined, amounts to a total of 100%, providing a comprehensive representation of the event detection and non-detection. The detailed chart of the overlap criteria is included in SI 1.6.

Using Stanford-defined events as a baseline allows us to ask: when gas is released onsite, does the continuous monitoring solution identify an emission? Using the team-defined events as a baseline allows us to ask the inverse question: when the system identifies an emission event, was gas being released onsite? For an ideal system, these two metrics will converge: all events detected by the system will be Stanford release events, defined as ground truth events shown in Figure 2. Using these two methods, we calculate the following metrics for each system.

- **Detection Rate (TP/(TP+FN)%):** The percentage of Stanford emissions correctly identified.
- **Non-Emission Accuracy (TN/(TN+FP)%):** The percentage of correctly identified Stanford non-emission periods.

- **Emission Identification Reliability (TP/(TP+FP)%):** The percentage of team-reported emissions that were correctly identified.

- **Non-Emission Identification Reliability (TN/(TN+FN)%):** The percentage of team-reported periods correctly identified as non-emission.

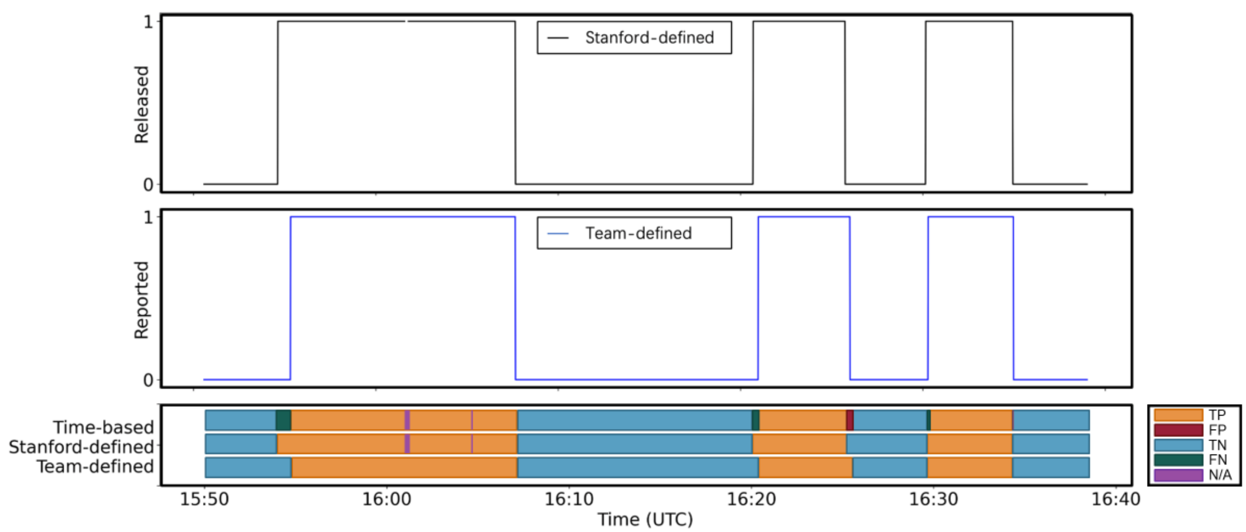

Figure 2: Event matching comparison for a team on October 30, 2022, from 15:50 to 16:40 UTC. The upper section displays events as defined by Stanford, while the middle section showcases binary events reported by continuous monitoring teams, which indicate the presence or absence of emissions. The lower section presents classifications based on Stanford-defined, team-defined, and time-based rules. Distinct colors, detailed at the bottom of the graph, demarcate these classifications. TN = True Negative, TP = True Positive, FN = False Negative, FP = False Positive, using time-based and event-based metrics. See Methods for additional details. Any events reported by the team that coincide with these filtered periods are labeled as "N/A".

Event-based metrics quantify emission detection occurrences, treating short and long detections equally. For example, detecting any part of a 60-minute emission event is counted the same, whether the detection lasts 10 minutes or 55 minutes. In contrast, time-based metrics evaluate how long emissions are accurately detected, offering a detailed measure of a system's performance over the event's duration. Therefore, a system that detects emissions for a longer period, such as 55 minutes out of 60, is considered more effective.

Combining these approaches provides a comprehensive assessment of monitoring performance. Event-based metrics determine the system's ability to detect emissions, while time-based metrics gauge how well it can continuously monitor them. This dual perspective ensures a robust evaluation of the technology's overall capabilities in continuous emission monitoring.

Due to SOOFIE's approach of reporting a block of 15-minute average for site-level emissions without detailing event duration, the event-based evaluation metric does not apply to the system and thus was not included in this portion of the analysis.

Evaluating quantification capabilities

Continuous monitoring solutions evaluate emissions over an extended period and have been proposed as an option for improving emission inventories.[23,41] For this reason, we focused on evaluating quantification by comparing Stanford's daily average emission rate to those reported by continuous monitors. Higher time resolution quantification estimates from these systems are generally noisy and difficult to interpret, as shown in figure 18 in SI 2.2.

To calculate the daily average emission rate, we defined the start and end times of each test date, using valid testing intervals and excluding the internal testing periods described above. We then determined the mean release rate over the relevant testing period, including periods of non-emissions. Notably, we did not include non-emission periods outside these intervals, such as overnight times, which were considered in our detection assessment.

Uncertainty in our quantification is determined using the uncertainty associated with gas measurement and methane mole fraction.[35] While the variability of the gas flow rate was high for any given day of testing, our calculations on the mean are precise and have a low uncertainty due to precision in the gas metering system, with 95% confidence intervals within $\pm$ 1.87%. For an in-depth understanding of these calculations, refer to SI 2.2.5. Oiler, Qube, and Sensirion provided calculated release uncertainties, whereas other teams did not. The uncertainty of quantification assessment for Project Canary was specifically conducted during the short stack height deployment phase.

We used continuous monitoring solutions reported-event data to calculate the daily average emissions rate for the relevant testing period only. Because systems may have picked up on the gas release from Stanford internal testing, which is excluded from the official testing period, we could not simply average all team-reported values for a given day.

Results

Here, we first describe the detection performance of the 8 continuous monitoring solutions, evaluated using both time-based and event-based metrics. Supplementary detection results are shown in SI 2.1. We then present the quantification results from all teams that reported quantification estimates. For an individual team's quantification performance, refer to SI 2.2.

During the official 45-day testing period, we logged 906 hours of testing. This includes known zero-emission times on usually nights and weekends. Gas releases also occurred at varied intervals throughout the week, including during the night, early morning, and weekend hours. There were some releases only separated by 5-minute long non-release periods, while others were more sporadic with days between events. Because we include all non-emission periods throughout the 2-month period, this corresponds to 9.34% of the entire released testing time(Figure 3). The release rate is presented with an error bar, which includes a 95% confidence interval, shown within brackets. The lowest instantaneous release rate was 0.037 [0.037, 0.037] kg CH_4/hr, and the highest was 2,830.211 [2619.50, 3040.93]kg CH_4/hr.

During the testing period, for point sensor networks, there were 107 emission events as defined by Stanford after using the wind transport model, with the shortest lasting 1.15 minutes. This event had release rates ranging from 0.776 to 4.95 kg CH_4/hr, with an average release emission of 2.27 [2.27, 2.27] kg CH_4/hr. The event with the largest range of releases lasted for 248 minutes, with the rates spread from 0.95 to 1,716.91 kg CH_4/hr and an average release of 427.95 [420.05, 435.86] kg CH_4/hr. There were also 147 Stanford-defined non-release periods. The duration between these non-release events varied, ranging from as short as 1.02 minutes to as long as 1,439.98 minutes. The most extended interval without emissions spanned 114.23 hours, starting from 22:10 on November 23, 2022 to 16:24 on November 28, 2022 in UTC. This period without emissions coincided with the Thanksgiving holiday in the United States.

For camera-based continuous monitoring solutions, there were 237 Stanford-defined emission events and 167 non-release periods. Events are defined by the start and end times of emissions. The event with the smallest range of releases was 1.00 minutes long, with an average release rate of 0.59 [0.59, 0.59] kg CH_4/hr. In contrast, the event with the largest range of releases was 213.95 minutes long, with releases spanning from 3.782 to 236.55 kg CH_4/hr, and the average release emission was 101.48 [101.08, 101.88] kg CH_4/hr.

Daily average release rates varied throughout the testing period as well. On November 30, 2022, the highest average daily release rate was recorded at 962.47 [945.70, 979.24] kg CH_4/hr. In contrast, on November 3, 2022, there was a wide range of releases observed, ranging from 18.49 to 2,830.21 kg CH_4/hr. The average release rate for this day was 812.54 [798.46, 826.62] kg CH_4/hr. The lowest average daily release rate was observed on November 14, 2022, at 28.4 [28.34, 28.46] kg CH_4/hr.

Time-based detection

Time-based detection shows the second-by-second comparison between Stanford methane releases and team-reported emissions. Figure 3 presents the time-based detection performance across the 8 continuous monitoring solutions. The 8 systems are grouped into two primary categories: camera-based technologies, which include Andium, Kuva, and Oiler, and point sensor networks represented by Project Canary, Ecotec, Qube, Sensirion, and SOOFIE. The sample sizes for these teams span a range from 914,142 to 3,128,980 measurement seconds (shown in Table 1). This is attributed to the differences in technology deployment and testing periods, as well as the duration when the systems were online, which resulted in the actual emitting time out of total time ranging from 8.39% to 35.51% (shown in SI 2.1). Each sample corresponds to a 1-second binary measurement as defined by the Stanford research team, indicating the presence or absence of gas emissions, alongside the detection classification (shown in figure 3a).

Both true positive and true negative rates are desirable to be higher metrics, as shown in figure 3b. The true positive rate or the proportion of accurately identified non-zero emissions, is a crucial performance metric. A high true positive rate suggests that the technology can correctly identify instances when emissions are occurring. True positive rates range from 9.7% (Ecotec) to 96.2% (Project Canary). Among the camera-based technologies, Andium registers a true positive rate of 57.6%, Oiler at a rate of 55.6%, and Kuva has a rate of 82.4%.

The true negative rates represent proficiency in correctly identifying periods without emissions. Both categories of systems registered true negative rates above 90%. The camera-based systems, namely Andium, Kuva, and Oiler, recorded true negative rates of 99.84%, 98.47%, and 99.75%, respectively.

Both false positive and false negative rates are desirable to be lower metrics. False positive rates represent the likelihood of generating false alarms. Across all teams, false positive rates are generally low. SOOFIE and Sensirion have slightly elevated rates at 8.7% and 2.7%, respectively. SOOFIE's reporting strategy, which reports average emission rates over 15-minute intervals, sometimes overlaps with non-emission periods. On the other hand, Sensirion's methodology, which reports events that often span entire testing days, cannot differentiate between emission and non-emission periods.

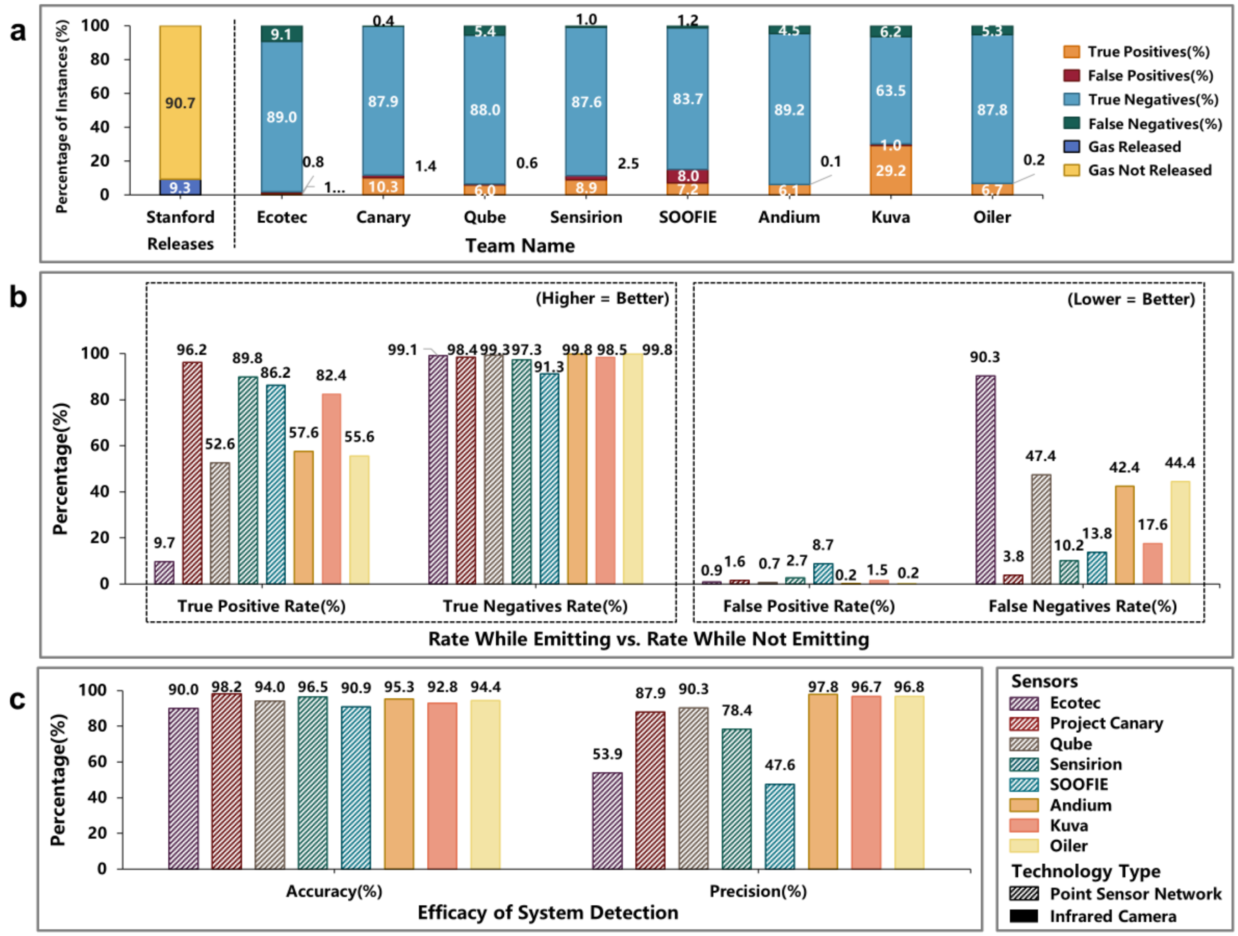

Figure 3: Time-based detection result for continuous monitoring systems. For all sub-plots, each bar represents a different sensor, and in sub-plots b and c, color indicates the specific sensor while the fill pattern indicates technology class (hash for point sensor network, solid for infrared camera). a) Results classification breakdown for the entire testing period. The left-most bar shows the proportion of the total testing period for which Stanford was releasing gas or not releasing gas. The remaining bars represent the total testing period for each participant, broken down by proportion of true positives (gas released and detected), false negatives (gas released but not detected), true negatives (no gas released and correctly identified), and false positives (no gas released but incorrectly identified as released). b) Performance metrics using time-based evaluation. Participant performance was evaluated using true positive rate, true negative rate, false positive rate, and false negative rate. For the metrics on the left, stronger performance is indicated by values closer to 100%. For the metrics on the right, stronger performance is represented by values closer to 0%. c) Efficacy of system detection using time-based evaluation. Accuracy indicates how often the sensors correctly identified whether gas was released or not, and precision is the percentage of true positives against all sensor-reported positive readings. See Methods for additional details.

The false negative rate measures how often a system fails to detect actual emission events. A high false negative rate implies frequent misses in detection. There is a significant variation in the false negative rates among the teams, even within their respective categories. Among the camera-based technologies, the false negative rate ranges from 17.6% to 44.4%. Among point sensor networks, Project Canary's detection had a false negative rate of 3.8%. However, this appears to be an artifact of Canary's reporting approach, in which they typically report one long extended event. It is also notable that Project Canary's sample size is reduced compared to the other point sensor networks since they are evaluated solely on a short-release stack. Ecotec had a false negative rate of 90.3%. Likewise, this result is affected by their reporting approach, which typically consists of short-duration events that range from seconds to 7 minutes, leading them to miss continuous emissions released by Stanford. Such variations underscore the different efficacy levels of the teams in pinpointing actual emissions, and also the difficulty of encapsulating performance in a single metric.

Evaluating system performance requires a focus on both accuracy and precision (shown in figure 2c), as these metrics offer a more informative view of a system's reliability. Accuracy represents the system's overall ability to correctly classify periods (proportion of true positives and true negatives out of the total sample size).

Teams tend to record high true negatives because we include periods, such as nights and weekends, when usually no emissions are released. While all systems consistently achieve an accuracy rate above 90%(summarized in figure 3a), the high accuracy may be influenced by a large number of true negatives. The nature of our study, which focuses on releasing intermittent high-volume emissions, may also contribute to high true negatives since there are gaps in emissions during the operational period. Consequently, while the high accuracy rate underscores the systems' robust performance in time-based evaluations, it is important to consider other metrics, such as precision, to fully assess the system's effectiveness in distinguishing between emission and non-emission periods.

Precision represents the system's proficiency in accurately identifying emission events while minimizing false positives (the proportion of true positive measurements out of the sum of true positives and false positives). This metric becomes paramount in contexts where high precision translates to reduced false alarms, thus averting unwarranted and expensive investigations. Among the camera-based systems, Andium, Kuva, and Oiler achieve precision rates over 95%. Among point sensor networks, Qube has a precision of 90.3%. Such high precision indicates these systems can be trusted to detect true emission events with minimal errors on a second-by-second basis.

The precision of systems is influenced by the types of events they report and the duration of reported events. The lower precision rates for SOOFIE (47.6%) and Ecotec (53.9%) suggest a higher likelihood of false alarms. As mentioned above, Ecotec's methodology may result in fewer true positives when the system reports short emission events that do not overlap with Stanford-defined long-duration events. SOOFIE's 15-minute reporting format may inadvertently include non-emission intervals, leading to more false positives. This happens because the system does not provide high enough resolution to differentiate between actual emissions and background readings in its second-by-second comparison. These examples demonstrate how a system's reporting style can introduce variability in performance regardless of the metrics for evaluation. Hence, the results of the time-based analysis alone should be interpreted considering different contexts, and we provide the event-based analysis below to provide additional information on system performance.

Event-based detection

While the time-based analysis provides a continuous second-by-second analysis of detection capabilities, the event-based approach focuses on the system's ability to identify an emissions event at some point while it is occurring. A system that reliably detects using this approach can allow oil and gas operators to more effectively target their responses to emission alerts.

Figure 4 presents results for event-based detection. Four metrics are based on the definitions below. To avoid confusion with the time-based detection metrics, we use the following terminology: detection rate, non-emissions accuracy, reliability of identifications, and reliability of non-emission identifications. The detection rate evaluates whether a system correctly flags a Stanford emission event while gas is being released. For point sensor networks, it ranges from 25.6% to 95%. Among camera-based systems, Kuva has a 91.9% rate, and both Andium and Oiler are below 70%. Building on the observation that higher average wind speeds adversely affect continuous monitoring solutions' performance (as shown in SI 2.1), the range in detection rates demonstrates the variability in performance across solutions and the fact that many solutions still fail to identify a large proportion of Stanford emission events.

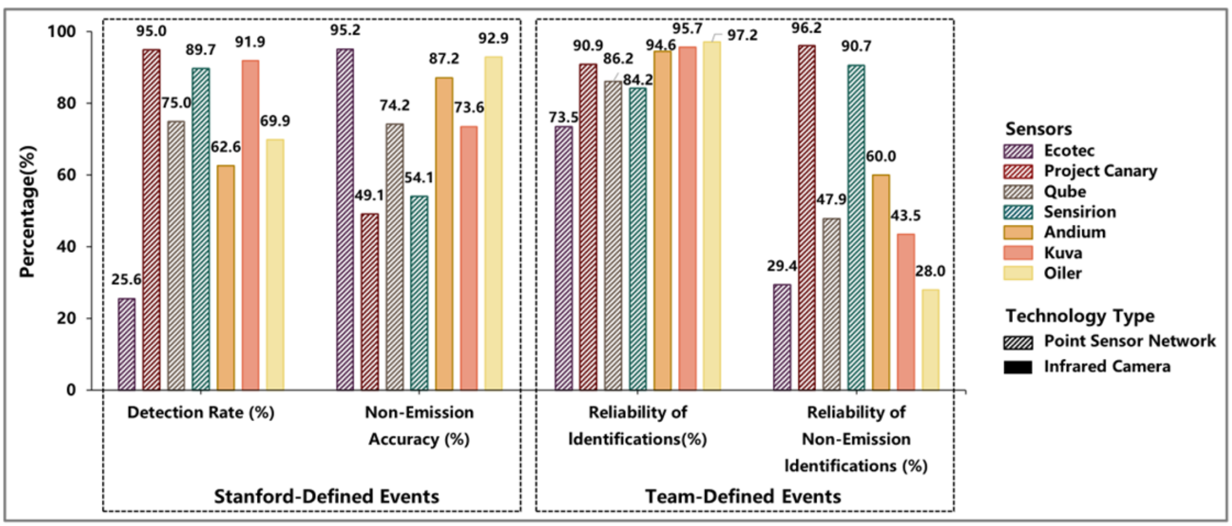

Figure 4: Event-based detection results from continuous monitoring systems. In all cases, stronger performance is indicated by results closer to 100%. Bars are colored based on the participant, and the fill pattern indicates the technology type (hash for point sensor network, solid for infrared). Stanford-defined events (left panel) assess whether the monitoring system accurately detects emissions when Stanford releases gas, using the metrics detection rate and non-emission accuracy. Detection rate is the proportion of all emission events correctly classified as true positive (TP/(TP+FN)), and non-emission accuracy is the proportion of all non-emission events correctly classified as true negatives (TN/(TN+FP)). Team-defined events (right panel) examine a system's precision in real-world conditions, evaluating whether reported emissions correspond to actual onsite gas releases with the metrics of reliability of emission identification and non-emission identification. Reliability of identification is the proportion of team-reported emission events that were correct (TP/(TP+FP)), and reliability of non-emission identification is the proportion of team-reported non-emission events that were correct (TN/(TN+FN)).

Non-emission accuracy is the measure of the systems' ability to correctly identify periods without emissions. This metric evaluates the precision in differentiating between ambient environmental conditions and actual emission events. Our study encompassed both long- and short-emission events. More than 24% of total zero-emission periods were less than 10 minutes. Therefore, when deciding which solution to use, oil and gas operators should consider which types of emission events they want to monitor. The system performance in this category varies widely. Over half the system can correctly identify true non-emission events more than 74% of the time when no gas is released.

Reliability of identification provides a metric of how frequently a system alert in turn aligns with an actual emission event. Here, Oiler remains consistent with a leading score of 97.2%. Ecotec is at 73.5%. However, performance in this category is notably high. Likewise, the reliability of non-emission identification indicates the extent to which a system accurately reports periods of non-emissions, without false alerts. Project Canary has a reliability of identification of 96.2%. Oiler has 28%. Figure 4 reveals significant variability in system reports when no gas is present onsite.

Event-based evaluations reveal the complexity of choosing a specific methane detection system. Qube technology, for example, has high reliability in emission identification but less so in recognizing non-emission periods. On the other hand, Project Canary has a high detection rate but has a relatively low non-emission accuracy. These varied performances highlight the value of adopting a comprehensive evaluation approach. By integrating these metrics, stakeholders can assess both the detailed performance of systems in real-time monitoring (time-based) and their effectiveness in identifying discrete emission events (event-based). They can use this integrated approach to tailor their selection of monitoring systems based on specific operational needs. For a detailed analysis and understanding of these metrics, please refer to the "Discussion" section of our paper.

Quantification

In the assessment of daily average release quantification, four sensor networks (SOOFIE, Sensirion, Project Canary, and Qube) and one camera-based technology (Oiler) were involved, as shown in Figure 5. This figure compares daily average metered release rate in kg(CH_4)/hr with reported daily average emission estimates for each participating team, using ordinary least square (OLS) regression to analyze the relationship. OLS is appropriate here because the errors in the x-direction are much smaller than the errors in the y-direction. Other than SOOFIE, all other 4 systems have reported uncertainty data.

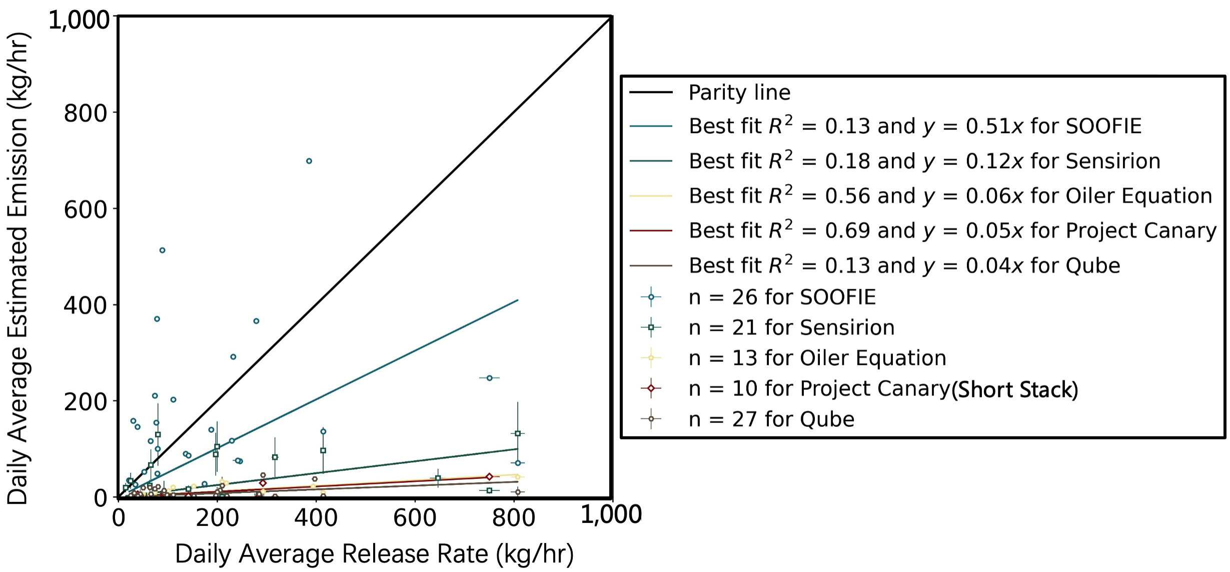

Figure 5: Daily average quantification plot for systems: The x-axis of the graph represents the daily average methane release rate recorded by Stanford, with error bars depicting the 95% confidence interval (CI), which may not be visible due to their small magnitude. The y-axis is the daily average release rate reported by the continuous monitoring solutions, with error bars reflecting the reported 95% CI uncertainty for all participants except SOOFIE who did not report uncertainty. The black line x=y line indicates parity. Data from each system or team is presented in distinct colors for clear differentiation.

Following a request from Project Canary before the testing phase, we evaluated their 10 samples specifically during the short stack height period. This achieves an R^2 value of 0.69 and a slope of 0.05. In contrast, the other four systems were assessed over both short and tall stack height scenarios. Slopes range from 0.04 to 0.12, indicating different levels of sensitivity to the metered release rates. R^2 values range from 0.13 to 0.69, reflecting a wide variation in the accuracy of the systems' readings. The graph depicting the short stack height scenario for the rest of the four systems can be found in SI 2.2.

The observed downward bias trend among these systems, shown in figure 5, suggests that these systems tend to report lower emissions than the metered rates, underscoring the challenges associated with precise methane emission quantification using continuous monitoring systems.

Discussion

In this study, we evaluated methane detection and quantification technologies over a 45-day testing period. This study was notable for its inclusion of larger methane sources similar to those seen in large-scale equipment failures, unlit flares, and tank emission control failures. These emission sources are often called "super-emitters." In addition, the sensor deployment by participants generally reflects their standard practices for oil and gas operator sites of comparable sizes, as reported by participants. See SI 1.1 for more details.

In the real world, oil and gas operators have dual needs for detection capability. One is for immediate alerts to quickly respond to methane leaks and events, and the other is to have accurate measurements of emission duration and size for regulatory compliance. Our study takes into account both needs and therefore the results need to be considered in a nuanced fashion.

Results suggest that at least some of the systems can quite effectively detect the existence of large emissions sources. The resulting performance supports these systems' capacity to function as an early warning system, akin to a fire alarm, that will signal when a large failure event happens. However, these systems tend to imperfectly or poorly estimate the duration or precise timing of an emission event.

For instance, a system might show a high detection rate in the event-based analysis because it successfully identifies most emission events at some point during their occurrence. However, the same system might have a lower TP rate in the time-based analysis if it fails to detect the emissions consistently throughout the event duration. Based on the application-specific priorities of the reader, one metric thus may be more useful than another. For developing emissions inventories, it may be more important to have a system that performs well in time-based detection, providing a more accurate depiction of how long a leak lasts or its intermittency. However, for leak detection and repair, a facility manager may prioritize a solution that can accurately identify events allowing for an immediate response, regardless of the system's performance in the time-based metrics.

Examining results for specific teams can better illustrate this point. For example, Project Canary's approach, characterized by reporting prolonged events with intermittent gaps, achieved a detection rate of 95%, indicating a proactive stance towards emission detection. However, this approach resulted in a lower non-emission accuracy of 49.1%, potentially leading to over-reporting of events. Such a design may necessitate additional verification by oil and gas operators, which can be resource-intensive. Conversely, Oiler's method, marked by distinct reporting of emissions and non-emissions events, led to a non-emission accuracy of 92.9%. This precision in identifying true emission events aids in targeted maintenance and compliance reporting. However, its detection rate of 69.9% suggests that this technology may miss a substantial fraction of emission events.

In addition to the disparate results in these examples, an interesting observation arises when the criteria for an overlap rate are adjusted. When the time overlap threshold is tightened from 10% to 50% of the release time in seconds for all positive events (as detailed in SI 2.1), the detection rate of the four systems under study drops below 60%. Furthermore, we found that for some tested participants, the detection rate of continuous monitoring solutions decreases as the average wind speed increases throughout the experiment (as detailed in Figure 13 in SI 2.1). There is also a trend of improved performance from the systems with increasing release rates (as detailed in Figure 11 in SI 2.1). Future studies would be helpful to examine the detection capabilities of continuous monitoring systems in relation to high-volume releases under variable wind conditions.

Our results indicate that continuous monitoring solutions could be improved to provide alerts that accurately align with both the start and end of actual emission events. This would provide a more precise and reliable monitoring process.

Quantification performance is poor and requires immediate improvement if these sensors are to be deployed for methane measurement. As shown in figure 5, there are significant discrepancies in the average reported emission rate, evident through the strong downward bias in all linear regression slopes. Additionally, the high degree of scatter in the data is evident through the R^2 values that range from 0.13 to 0.69. Our findings spotlight the difficulties continuous monitoring solutions encounter in accurately quantifying methane emissions. The strong downward bias could lead oil and gas operators to inadvertently rely on data that underestimates their actual environmental impact, while also misrepresenting their compliance with regulations. Consequently, oil and gas operators who currently use these sensors for emissions tracking and reporting may need to re-evaluate this approach. Given that only 5 out of 8 companies opted for quantification evaluation (as shown in table 1), there is a clear need for more research and development to improve sensor performance. This is particularly the case when we compare to airplane-based detection methods which exhibit excellent quantification ability.[35]

It is important to highlight the limitations of this study. Firstly, the testing environment was selected with an emphasis on simplicity to facilitate clear and interpretable source detection. For instance, we chose a location with minimal confounding methane sources, devoid of significant wind obstructions, and characterized by a uniform, flat terrain. While this is advantageous for clear testing purposes, it does not accurately represent all operational terrains. In more complex environments, technologies could exhibit different performances, underscoring the importance of diverse testing scenarios.

Secondly, there is a possibility that test participants might deduce the characteristics of the testing regime. Given that a Stanford field team member needs to be on-site to control emissions, there are somewhat predictable periods of zero emissions, such as overnight and on weekends. These periods could have influenced the overall performance metrics. For instance, test participants might deduce that emission sources at 3 a.m. are unlikely in our study design and consequently remove false positives from those periods. Nonetheless, this kind of reasoning may not be entirely detached from actual operational scenarios. In real-world settings, emission events are often sporadic and tied to human activity, as was the case in the study.[9] Therefore, while such assumptions might affect the study's findings, they also reflect realistic patterns that could occur in practical applications of methane detection systems.

Lastly, the source location in our study is predetermined. This scenario is similar to real-world situations where the position of a tank battery or flare stack is known in advance so that sensors can be set up near these likely sources. However, this design doesn't represent cases where emissions could emanate from any one of numerous small equipment pieces, connectors, or flanges across a large facility. For such smaller dispersed leaks, the results from the METEC testing of continuous monitors offer a more accurate representation.[23,42]

Our study, which complements the METEC findings, offers additional insights on large-source emission detection and quantification.[23,41,42] While METEC had anonymized participant data, we directly connected results to individual teams. Furthermore, while METEC's experiments focus on multiple smaller methane leaks (< 25 kg/hr) from a wide range of possible sources, our work encompasses larger emissions from a single source (< 1600 kg/hr). Note that in a study that more closely mimics real-world conditions, Day et al. observed a significant deterioration in detection performance compared to the more controlled setup at METEC.[41] This comparison highlights the difficulty continuous monitors face in accurate detection, particularly when moving from controlled environments to more complex, real-world scenarios. Our work concentrates on measuring the capacity for detecting and quantify high-volume emission events from a single point source. Both METEC and Stanford approaches reveal critical uncertainties in single-source emission estimations, which are essential to refine the accuracy of greenhouse gas inventories.[43]

Overall, we find continuous monitoring systems succeed as early warning devices for detecting large methane emissions in the oil and gas sector. Yet, when it comes to detailed assessments of emission duration and volume — key for meeting regulatory and environmental standards — these systems must be improved. Our research points to specific challenges in maintaining detection over time and accurately quantifying emissions. Given the desire for more measurement-based inventory methods, caution should be used when applying these kinds of measurements to inventory generation.

The journey to refine continuous monitoring solutions for GHG inventory accuracy is ongoing. Future enhancements and tests will depend on sustained research and development, and a collaborative approach among researchers, industry stakeholders, and regulators. This study helps us understand the capabilities and limitations of current monitoring technologies, guiding the path toward more reliable and precise environmental monitoring and reporting.

Code availability

Code supporting the current study is available at: https://github.com/Richardczl98/2022-Control-Release–Continuous-Monitoring

Acknowledgments

This research was funded by the Environmental Defense Fund, Global Methane Hub, International Methane Emissions Observatory, and the Stanford Natural Gas Initiative, an industry consortium at Stanford. We thank the operational team for their support and coordination. **Andium:** Mark Davis and Alexander Ayala. **Canary:** Will Foiles and Kieran Lynn. **Ecotec:** Alan Vidal, Jamie Tooley, Mitch Cassel and Tim Novick. **Kuva:** Jason Bylsma, Thomas Mcarthur, and Stefan Bokaemper. **Oiler:** Ziliang Mao and Bo Fu. **Qube:**

Eric Wen, Everett Robinson, and Greg Taylor. **Sensirion:** Susanne Pianezzi, Scott Newell, Ryan Fitzpatrick, Dominik Niederberger and Patrick Ploesser. Rawhide Leasing and Volta Fabrication, especially Mike Brando, Walt Godsil and S.M., offered operational support. C. Kocurek advised on experimental design, while Thuy Nguyen and Cerise Burns managed administrative tasks. We thank Long Zhou for the GitHub support and guidance. Thanks to the Creative Café and Mi Amigo Ricardo for catering to the Stanford team's dietary needs.

Author Contribution

Conceptualization –Z.C, S.H.E., E.D.S., A.R.B. Methods –Z.C, S.H.E., E.D.S., A.R.B. Software – Z.C, S.H.E., P.M.B. Validation – Z.C, S.H.E. Formal analysis –Z.C. Investigation – S.H.E., Z.C., J.S.R., Z.Z., Y.C., E.D.S., P.M.B. Data Curation –Z.C., S.H.E., P.M.B. Writing Original Draft –Z.C, S.H.E. Writing–Review & Editing –all authors. Supervision – Z.C, S.H.E., A.R.B., Project administration –S.H.E., E.D.S., A.R.B.. Funding acquisition–S.H.E., E.D.S., A.R.B.

Competing Interest

J.S.R. is currently employed by Highwood Emissions Management but was an affiliate of Stanford University when contributing to the current study. All other authors have no competing interests to declare.

References

(1) *Climate Change 2022 – Impacts, Adaptation and Vulnerability: Working Group II Contribution to the Sixth Assessment Report of the Intergovernmental Panel on Climate Change*; Cambridge University Press, 2023.

(2) Inflation Reduction Act. Legislation, August 16, 2022; Available at: https://www.govinfo.gov/app/details/BILLS-118hr812ih.

(3) Ocko, I. B.; Sun, T.; Shindell, D.; Oppenheimer, M.; Hristov, A. N.; Pacala, S. W.; Mauzerall, D. L.; Xu, Y.; Hamburg, S. P. Acting rapidly to deploy readily available methane mitigation measures by sector can immediately slow global warming. *Environmental Research Letters* **2021**, *16*, 054042.

(4) Smith, S. J.; Chateau, J.; Dorheim, K.; Drouet, L.; Durand-Lasserve, O.; Fricko, O.; Fujimori, S.; Hanaoka, T.; Harmsen, M.; Hilaire, J.; others Impact of methane and black carbon mitigation on forcing and temperature: a multi-model scenario analysis. *Climatic Change* **2020**, *163*, 1427–1442.

(5) IEA Methane Tracker 2021. 2021; https://www.iea.org/reports/methane-tracker-2021, License: CC BY 4.0.

(6) Ravikumar, A. P.; Roda-Stuart, D.; Liu, R.; Bradley, A.; Bergerson, J.; Nie, Y.; Zhang, S.; Bi, X.; Brandt, A. R. Repeated leak detection and repair surveys reduce methane emissions over scale of years. *Environmental Research Letters* **2020**, *15*, 034029.

(7) Golston, L. M.; Aubut, N. F.; Frish, M. B.; Yang, S.; Talbot, R. W.; Gretencord, C.; McSpiritt, J.; Zondlo, M. A. Natural gas fugitive leak detection using an unmanned aerial vehicle: Localization and quantification of emission rate. *Atmosphere* **2018**, *9*, 333.

(8) Kemp, C. E.; Ravikumar, A. P. New technologies can cost effectively reduce oil and gas methane emissions, but policies will require careful design to establish mitigation equivalence. *Environmental Science & Technology* **2021**, *55*, 9140–9149.

(9) Cusworth, D. H.; Duren, R. M.; Thorpe, A. K.; Olson-Duvall, W.; Heckler, J.; Chapman, J. W.; Eastwood, M. L.; Helmlinger, M. C.; Green, R. O.; Asner, G. P.; others

Intermittency of large methane emitters in the Permian Basin. *Environmental Science & Technology Letters* **2021**, *8*, 567–573.

(10) Wik, M.; Thornton, B. F.; Bastviken, D.; Uhlbäck, J.; Crill, P. M. Biased sampling of methane release from northern lakes: A problem for extrapolation. *Geophysical Research Letters* **2016**, *43*, 1256–1262.

(11) Vaughn, T. L.; Bell, C. S.; Pickering, C. K.; Schwietzke, S.; Heath, G. A.; Pétron, G.; Zimmerle, D. J.; Schnell, R. C.; Nummedal, D. Temporal variability largely explains top-down/bottom-up difference in methane emission estimates from a natural gas production region. *Proceedings of the National Academy of Sciences* **2018**, *115*, 11712–11717.

(12) Plant, G.; Kort, E. A.; Brandt, A. R.; Chen, Y.; Fordice, G.; Gorchov Negron, A. M.; Schwietzke, S.; Smith, M.; Zavala-Araiza, D. Inefficient and unlit natural gas flares both emit large quantities of methane. *Science* **2022**, *377*, 1566–1571.

(13) Regan, M. S. Standards of Performance for New, Reconstructed, and Modified Sources and Emissions Guidelines for Existing Sources: Oil and Natural Gas Sector Climate Review. Environmental Protection Agency, 2023; https://www.regulations.gov/docket/EPA-HQ-OAR-2021-0317/documents, Final rule. Docket No. EPA-HQ-OAR-2021-0317; FRL-8510-01-OAR; RIN 2060-AV16. Effective [60 days after publication in the Federal Register].

(14) Allen, D. T.; Cardoso-Saldaña, F. J.; Kimura, Y. Variability in spatially and temporally resolved emissions and hydrocarbon source fingerprints for oil and gas sources in shale gas production regions. *Environmental Science & Technology* **2017**, *51*, 12016–12026.

(15) Fox, T. A.; Barchyn, T. E.; Risk, D.; Ravikumar, A. P.; Hugenholtz, C. H. A review of close-range and screening technologies for mitigating fugitive methane emissions in upstream oil and gas. *Environmental Research Letters* **2019**, *14*, 053002.

(16) Titchener, J.; Millington-Smith, D.; Goldsack, C.; Harrison, G.; Dunning, A.; Ai, X.; Reed, M. Single photon Lidar gas imagers for practical and widespread continuous methane monitoring. *Applied Energy* **2022**, *306*, 118086.

(17) Wang, J. L.; Daniels, W. S.; Hammerling, D. M.; Harrison, M.; Burmaster, K.; George, F. C.; Ravikumar, A. P. Multiscale methane measurements at oil and gas facilities reveal necessary frameworks for improved emissions accounting. *Environmental science & technology* **2022**, *56*, 14743–14752.

(18) Chen, Q.; Modi, M.; McGaughey, G.; Kimura, Y.; McDonald-Buller, E.; Allen, D. T. Simulated methane emission detection capabilities of continuous monitoring networks in an oil and gas production region. *Atmosphere* **2022**, *13*, 510.

(19) Aboughaly, M.; Fattah, I. Environmental Analysis, Monitoring, and Process Control Strategy for Reduction of Greenhouse Gaseous Emissions in Thermochemical Reactions. *Atmosphere* **2023**,

(20) Agency, U. S. E. P. Leak Detection and Repair: A Best Practices Guide. 2007; Google Scholar. There is no corresponding record for this reference.

(21) Siebenaler, S. P.; Janka, A. M.; Lyon, D.; Edlebeck, J. P.; Nowlan, A. E. Methane detectors challenge: Low-cost continuous emissions monitoring. International Pipeline Conference. 2016; p V003T04A013.

(22) Ravikumar, A. P.; Sreedhara, S.; Wang, J.; Englander, J.; Roda-Stuart, D.; Bell, C.; Zimmerle, D.; Lyon, D.; Mogstad, I.; Ratner, B.; others Single-blind inter-comparison of methane detection technologies–results from the Stanford/EDF Mobile Monitoring Challenge. *Elem Sci Anth* **2019**, *7*, 37.

(23) Bell, C.; Ilonze, C.; Duggan, A.; Zimmerle, D. Performance of Continuous Emission Monitoring Solutions under a Single-Blind Controlled Testing Protocol. *Environmental Science & Technology* **2023**, *57*, 5794–5805.

(24) Sherwin, E.; Rutherford, J.; Zhang, Z.; Chen, Y.; Wetherley, E.; Yakovlev, P.; Berman, E.; Jones, B.; Thorpe, A.; Ayasse, A.; others Quantifying oil and natural gas system emissions using one million aerial site measurements. **2023**,

(25) Brandt, A. R.; Heath, G. A.; Cooley, D. Methane leaks from natural gas systems follow extreme distributions. *Environmental science & technology* **2016**, *50*, 12512–12520.

(26) Zavala-Araiza, D.; Alvarez, R. A.; Lyon, D. R.; Allen, D. T.; Marchese, A. J.; Zimmerle, D. J.; Hamburg, S. P. Super-emitters in natural gas infrastructure are caused by abnormal process conditions. *Nature communications* **2017**, *8*, 14012.

(27) Andium Andium: Homepage. 2023; https://www.andium.com/, Accessed: 2023-10-15.

(28) Ecotec Ecotec: Homepage. 2023; https://www.ecotecco.com/, Accessed: 2023-10-15.

(29) ChampionX Continuous Emissions Monitoring - SOOFIE. 2023; https://www.championx.com/products-and-solutions/emissions-technologies/continuous-emissions-monitoring-soofie/, Accessed: 2023-10-15.

(30) Equation, O. Oil Equation: Homepage. 2023; https://www.oilerequation.com/, Accessed: 2023-10-15.

(31) Systems, K. Kuva Systems: Homepage. 2023; https://www.kuvasystems.com/, Accessed: 2023-10-15.

(32) Canary, P. Project Canary: Homepage. 2023; https://www.projectcanary.com/, Accessed: 2023-10-15.

(33) IoT, Q. Qube IoT: Homepage. 2023; https://www.qubeiot.com/, Accessed: 2023-10-15.

(34) Connected, S. Emissions Monitoring. 2023; https://sensirion-connected.com/emissions-monitoring, Accessed: 2023-10-15.

(35) El Abbadi, S. H.; Chen, Z.; Burdeau, P. M.; Rutherford, J. S.; Chen, Y.; Zhang, Z.; Sherwin, E. D.; Brandt, A. R. Comprehensive evaluation of aircraft-based methane sensing for greenhouse gas mitigation. **2023**,

(36) Sherwin, E.; El Abbadi, S.; Burdeau, P.; Zhang, Z.; Chen, Z.; Rutherford, J.; Chen, Y.; Brandt, A. Single-blind test of nine methane-sensing satellite systems from three continents. *EGUsphere* **2023**,

(37) Aldhafeeri, T.; Tran, M.-K.; Vrolyk, R.; Pope, M.; Fowler, M. A review of methane gas detection sensors: Recent developments and future perspectives. *Inventions* **2020**, *5*, 28.

(38) Sun, S.; Ma, L.; Li, Z. Methane Emission Estimation of Oil and Gas Sector: A Review of Measurement Technologies, Data Analysis Methods and Uncertainty Estimation. *Sustainability* **2021**, *13*, 13895.

(39) Bell, C.; Zimmerle, D. METEC controlled test protocol: continuous monitoring emission detection and quantification. Ph.D. thesis, Colorado State University. Libraries.

(40) Henry, S.; Zimmerle, D. *Advancing Development of Emissions Detection (ADED)*; Project Report FE0031873, 2023.

(41) Day, R. E.; Emerson, E.; Bell, C.; Zimmerle, D. Point Sensor Networks Struggle to Detect and Quantify Short Controlled Releases at Oil and Gas Sites. *Sensors* **2024**, *24*, 2419, Submission received: 27 February 2024 / Revised: 1 April 2024 / Accepted: 7 April 2024 / Published: 10 April 2024.

(42) Ilonze, C.; Emerson, E.; Duggan, A.; Zimmerle, D. Assessing the progress of the performance of continuous monitoring solutions under single-blind controlled testing protocol. *ChemRxiv* **2024**, Preprint has not been peer-reviewed.

(43) Jonas, M.; Bun, R.; Nahorski, Z.; others Quantifying greenhouse gas emissions. *Mitigation and Adaptation Strategies for Global Change* **2019**, *24*, 839–852.

Supplementary Information for Comparing Continuous Methane Monitoring Technologies for High-Volume Emissions: A Single-Blind Controlled Release Study

Zhenlin Chen[1], Sahar H. El Abbadi[2], Evan D. Sherwin[2], Philippine M. Burdeau[1], Jeffrey S. Rutherford[a], Yuanlei Chen[1], Zhan Zhang[1], Adam R. Brandt[1]
[1]Energy Science & Engineering, Stanford University, Stanford, California 94305, United States
[a]Highwood Emissions Management, Calgary, Alberta T2P 2V1, Canada
[2]Lawrence Berkeley National Laboratory, Berkeley, California 94720, United States

Contents

S1 Supplementary Methods

1.1 Data reporting protocol

Our reporting methodology has been meticulously refined to align with the Advanced Detection Evaluation and Reporting (ADED) protocol, as established by the Methane Emission Technology Evaluation Center (METEC) in Colorado.[1,2] This protocol dictates a structured approach to data categorization and report generation for each emission event detected by continuous monitoring solutions.

To maintain consistency and comprehensive data capture, each detection report submitted by the participating teams includes essential fields such as “DetectionReportID” and “EmissionStartDateTime”. These mandatory fields allow for precise tracking and analysis of emission events. Additionally, our reporting system addresses the operational status of the monitors. Off-line reports, marked with “OfflineReportID” and “OfflineDateTime”, provide clarity on when monitors are non-operational, ensuring that our dataset reflects both active and inactive periods accurately.

Beyond these existing ADED requirements, our reporting framework incorporates new metrics for a more in-depth analysis of monitoring performance. We have introduced an “Alarm” column to indicate when conditions warrant notifying a customer, and a “Variable Confounding

Source" field to identify if emissions originate from outside the Stanford testing facility. These additions, along with the estimated "EmissionRate" reported in kilograms per hour, enable a more responsive and precise environmental monitoring system.

The deployment details and logistical parameters governing the placement and monitoring of sensor technology at the study site are concisely documented in Table 1. To maintain the integrity of the study environment, technicians from the participating monitoring companies were subject to specific restrictions regarding the placement of their equipment. Strict adherence to the designated safety perimeter, delineated by an orange line in Figure 1 of the main paper, was enforced, along with the stipulation that equipment could not be placed outside the confines of the demarcated zones, as indicated by the fence in the same figure.

Technicians were granted access to the site for routine visits under supervision, allowing them to check the continuous functionality of their equipment and carry out any necessary modifications. These routine checks and any subsequent alterations made to the setup of the monitoring equipment during the study are detailed for each sensor in Table 1.

Table 1: Sensor Deployment Information

Sensor Name	**Technology Type**	**Deployment Date (2022)**	**Number of Units**	**Typical Deployment Units**	**Total site visits**	**Notes**
Ecotec	Point sensor network	10/28 – 11/28	2	4	3	Setting up on 10/24 and 10/25 morning
Project Canary		10/10 – 11/29	8	4	2	Install and Uninstall
Qube		10/10 – 11/23	6	4 to 6	2	Install and Uninstall
Sensirion		10/10 – 11/30	6	4 to 8	3	Sensor blew by the sandstorm and reset on 10/8
SOOFIE		10/10 – 11/29	12	N/A	2	Install and Uninstall
Andium	Infrared camera	10/10 – 11/23	2	1	2	Install and Uninstall
Kuva		10/10 – 11/23	1	1	2	Install and Uninstall
Oiler		10/10 – 11/03	1	1 to 3	2	Install and Uninstall

1.2 Gas stack usage

The study utilized two vertical gas release stacks made of 6-inch diameter high-density polyethylene, measuring 20 feet and 6 feet in length. The gas was released at heights of 24 feet and 10 feet above ground level when the stacks were vertical. A rotating elbow allowed for horizontal positioning; however, in this study, the stacks were used only in their vertical configuration.

Initial tests used the 20-foot stack, with a gas slip on the short stack observed on October 26th through an infrared camera. The slip potentially began on October 20th, detectable at flow rates as low as 300 kg/hr, and consistently visible above 800 kg/hr. To mitigate leakage, the short stack was removed and sealed on November 1st and then swapped with the tall stack on November 14th. Methane slip occurred during tests with continuous monitoring teams informed, as detailed in Table 2.

In evaluating methane detection efficacy across different stack heights, two pivotal metrics are essential: the volume of release events recorded and the precision of detection rates. Figure 1 delineates the quantity of data captured by an array of sensors at two distinct elevations. It reveals that the taller 7.3-meter stack registered a greater number of events across most sensors since the Stanford team conducted more experiments on the tall stack height. Conversely, the short stack's lower figures were partly attributed to technical issues that were later rectified.

Table 2: Usage of tall vs short release stacks

Date (2023)	Stack configuration
October 10–20	Tall stack (no slip)
October 20–30	Tall stack (with slip)
October 31	Short stack (with tall stack slip)
November 1–14	Tall stack (short stack removed, no slip)
November 14–30	Short stack (tall stack removed, no slip)

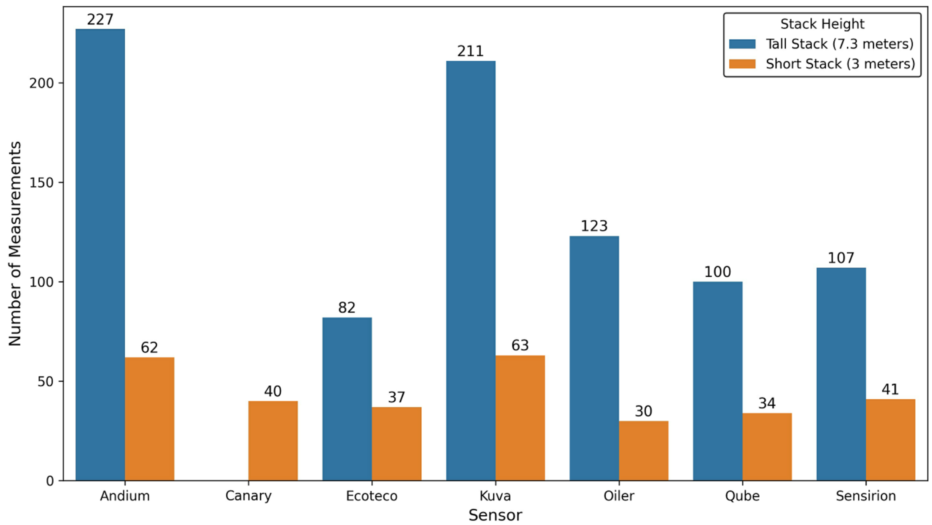

Fig 1: Stanford-defined events using two stack heights. The bar chart compares the number of release events from Stanford perspective that are evaluated for different sensors, distinguished by two stack heights: a taller one at 7.3 meters and a shorter one at 3 meters. The release events are different for each team due to different teams' employment periods for the experiment and system online and offline time. Each pair of bars represents a type of sensor. Canary only has one bar since the team is evaluated on short stack only.

Despite more frequent recordings at the tall stack, sensors generally demonstrated robust detection capabilities at both heights, as shown in Figure 2. The Andium sensor, for instance, although more active at the tall stack, registered a high detection rate at the lower elevation. The Canary sensor, evaluated solely at the short stack, exhibited high detection rates. This outcome highlights its strong performance, but without tall stack data, comparisons are incomplete.

Due to the gas leakage issue on the short stack, the releases by Stanford focus more on the tall stack. For a more equitable assessment of sensor performance, future studies should ensure a more balanced distribution of release events across both stack heights. This will facilitate a direct comparison, offering a clearer insight into each sensor's capabilities under equivalent conditions.

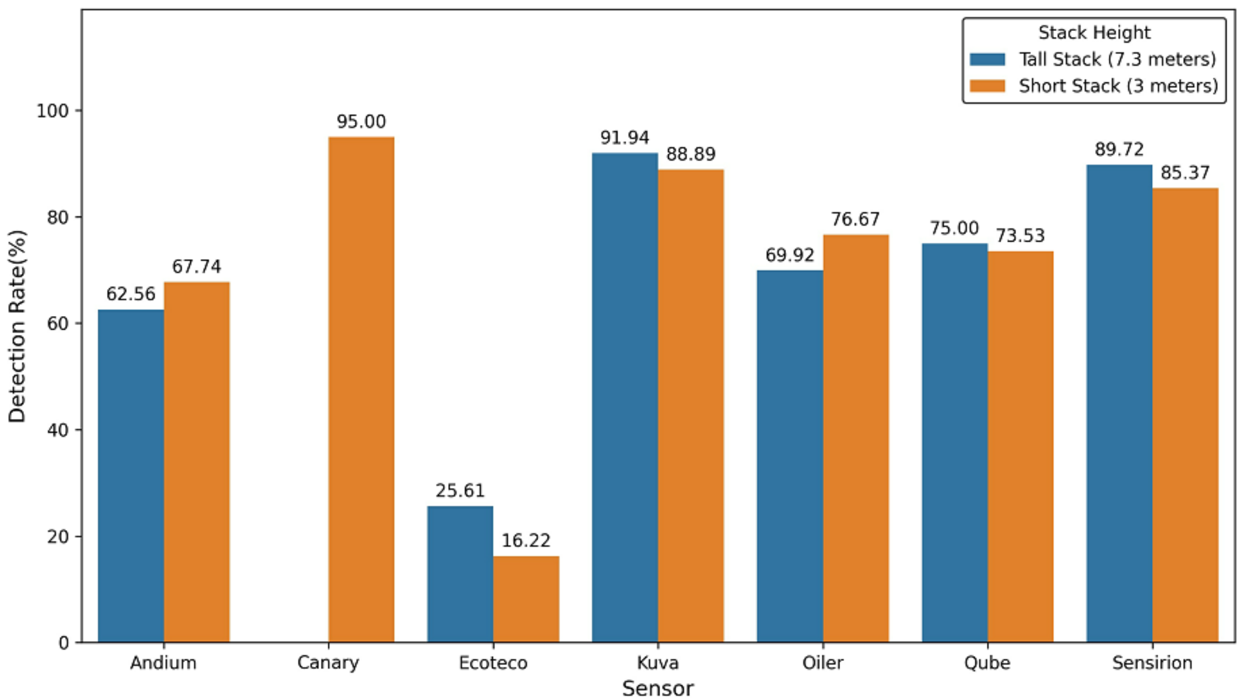

Fig 2: Stanford-defined event detection rate on different stack heights. The bar chart illustrates the detection rates (TP/(TP+FN)) of various sensors at two different stack heights: a tall stack at 7.3 meters and a short stack at 3 meters. The blue bars represent the detection rates at the tall stack, while the orange bars correspond to the short stack. Canary only has one bar since the team is evaluated on short stack only.

1.3 Data report from continuous monitoring solutions

Participants outlined their system configurations, including sensor types, equipment locations, and model numbers. Software versions and offsite analytic revisions crucial for data interpretation were also noted. Additionally, participants detailed survey metrics such as duration, altitude, confidence intervals, and personnel roles. For camera-based systems, plume length determination and wind speed integration methods were specified. Unreported periods were interpreted as non-detections, equivalent to 0 kg/hr.

Participants typically reported their sensor deployment strategies for a customer facility, closely matching the 4-acre size of our experimental field. The table 1 shows that the number of sensors deployed aligns with typical customer deployments of similar size. Participants indicate that the choice and number of sensors, as influenced by on-site equipment and wind conditions, directly affect emissions detection and distribution. The need for speed and accuracy in emission estimates determines the sensor quantity, with more sensors enhancing data precision and speed. However, while increased sensor density improves resolution, it also incurs higher costs and complex maintenance, alongside data management challenges. These factors must be carefully balanced to ensure an effective and sustainable sensor deployment strategy in real-world applications.

It is important to note that the Stanford team did not participate in the analysis of the reports submitted by the various teams. The data reporting template and the team's submitted raw data can be found on Github.

1.4 Participating continuous monitoring solutions

This section provides a summary of each commercial continuous monitor company details, testing equipment, sensor placements, and data submission timeline (Table 3).

We extended invitations to teams known for estimating methane emissions through continuous monitoring technologies. Those who chose not to participate are listed at the end of this section.

1.4.1 Andium

Company overview: Andium revolutionizes well-site management in the oil and gas sector. Their offerings encompass flare, tank, methane monitoring, asset tracking, liquid leak detection, and fire detection. These services aim to automate operational facets and guarantee a prompt reaction to on-site issues.[3]

Test equipment: For the test, the Andium AVS platform, featuring a 4K optical camera and optical gas sensor, was deployed. Positioned about 10 feet above ground, the device remained static throughout. The Andium Cloud platform (version 3) was employed for reporting and alerts. No meteorological or other sensors were used by Andium for this test.

Sensor location: Latitude: 32.823063, Longitude: -111.78568

1.4.2 Project Canary

Company overview: Project Canary offers enterprise emissions data solutions, empowering businesses to comprehend and mitigate their environmental footprint. Their portfolio includes emissions management, environmental risk evaluations, and advanced sensing devices for emission detection. Serving industries like upstream, midstream, utilities, and financial markets, they advocate for responsibly sourced gas and furnish platforms for methane intensity and climate attribute measurements. With operations in three countries, they have over 1,700 devices operational, logging over 760 million measurements monthly.[4]

Test equipment: 7 TLDAS sensors were arranged in a circle around the release points, positioned 1.5m above ground. Additionally, two anemometers were attached to the sensors on the North and West positions.

Sensor locations:

- East-Northeast: (32.821991, -111.785526)
- Northeast: (32.822135, -111.785749)
- Northwest: (32.822057, -111.786081)
- South: (32.821495, -111.785843)
- South-Southeast: (32.821414, -111.78556)
- Southwest: (32.821568, -111.78609)
- West: (32.821826, -111.786229)

1.4.3 Ecotec

Company overview:

Ecotec delivers monitoring and reporting solutions for greenhouse gas emissions, promoting safe and eco-friendly operations. Their portfolio combines hardware with integrated software, serving sectors such as landfill, biogas, wastewater, and oil & gas. Ecotec's unified platform comprises field-proven detection equipment and state-of-the-art software, aiming to meet regulatory standards and surpass ESG goals through real-time methane monitoring and comprehensive reporting.[5]

Test equipment: The Gazpod™ system from Ecotec features a patented tunable diode laser sensor with a closed herriott cell design. Gases are sampled using a pump-drawn method via the VEMM™ system, which collects from four different elevations: 5', 10', 15', and 20' above ground. For this study, a meteorological station was also situated on Unit 1, positioned east of the emission source.

Sensor locations:

- Unit 1: (32.821869, -111.785407)
- Unit 2: (32.8217889, -111.786233)

1.4.4 Kuva Systems

Company overview: Kuva Systems designs continuous methane monitoring, delivering actionable insights into gas emissions. They combine real-time, image-based methane emission alerts with their patented non-thermal infrared camera and cloud-based system. This platform ensures responses to emissions while streamlining operational processes and aligning with ESG goals. Their technology is applicable for varied contexts like well sites, compressor stations, and tank batteries, offering holistic monitoring solutions.[6]

Test equipment: Not specified.

Sensor locations: (32.821561, -111.785932)

1.4.5 Oiler

Company overview: Oiler delivers real-time methane monitoring solutions, blending affordability with effectiveness. Using their Optical Gas Imaging (OGI) camera, they pinpoint invisible gas leaks and support this with analytical tools and versatile cloud software. Their system is designed for diverse environments, from well pads to offshore platforms, streamlining compliance with emission goals and regulations.[7]

Test equipment: The company employed a fixed-mount, continuous monitoring OGI camera powered by solar energy. All detection and quantification were edge-processed without offsite software analytic. The camera's field of view spans 24 degrees horizontally and 19 degrees vertically.

Sensor locations: (32.82167, -111.78614)

1.4.6 Qube Technologies

Company overview: Qube Technologies provides solutions that combine hardware and physics-guided machine learning for continuous greenhouse gas emission monitoring. Their sensors are calibrated for the detection of methane and other gases. The integrated platform delivers real-time insights which are utilized for leak detection, repair management, and emissions reduction in various contexts. These solutions are designed to be cost-effective and are regulator-approved, making them suitable for a range of applications, from regulatory compliance to industrial odor management.[8]

Test equipment: The test equipment used was the AXON-V3, equipped with Qube AXON Firmware 3.10. It interfaces with the Qube Platform 2.0. This platform automatically manages data acquisition and analytics. Wind speed, measured by generic mechanical anemometers, is factored into the estimates of CH_4 mass flow for each device.

Sensor locations:

- AXON-V3-01802: (32.82196758, -111.7862418)
- AXON-V3-01805: (32.82127381, -111.785575)
- AXON-V3-01803: (32.82168365, -111.7852248)
- AXON-V3-01800: (32.82217583, -111.7855692)
- AXON-V3-01804: (32.82152925, -111.7862027)
- AXON-V3-01801: (32.82129045, -111.7859908)

1.4.7 Sensirion

Company overview: Sensirion Connected Solutions offers sensor-based monitoring solutions, specializing in continuous methane emissions monitoring for the energy sector. Originating from Stäfa, Switzerland, and with additional locations in Berlin and Chicago, the company has developed the Nubo Sphere technology. This technology efficiently detects, locates, and quantifies methane emissions, aiding energy companies in adhering to regulations and ESG standards. The solutions provided by Sensirion emphasize scalability, user-friendliness, and innovative sensor technology for emissions monitoring and predictive maintenance.[9]

Test equipment: The Nubo Sphere sensor network is designed for real-time methane emissions monitoring. It comprises three main components:

1.Sensor Hardware: The Nubo Sphere sensor node features two slots for sensing cartridges and an LTE connection for data transmission. The cartridges are exchangeable, and currently, a methane (CH_4) sensing cartridge using metal-oxide (MOx) technology is available. The nodes are autonomous due to solar panels, low-power electronics, and lithium-ion batteries. At least one node is equipped with a wind meter for local wind metrics.

2. Data Analytics: The system applies algorithms rooted in physical modeling to detect, locate, and quantify emissions in real time.

3. User Dashboard: The dashboard offers a real-time status of all sites, data visualization of emissions, and provides notifications for critical emission events. It's accessible via web browsers and smartphones.

All devices are positioned 2 meters above ground. The wind sensor is specifically installed at device cc1-27x7np-11-1c-16, with no additional meteorological data collected.

Sensor locations:

- cc1-03fvnp-15-46-38: (32.8221400, -111.7858810)
- cc1-03fvnp-15-47-39: (32.8221470, -111.7856290)
- cc1-03fvnp-16-30-38: (32.8214190, -111.7856600)
- cc1-03fvnp-18-32-11: (32.8219030, -111.7862320)
- cc1-27x7np-11-1c-16: (32.8217470, -111.7851870)
- cc1-27x7np-11-48-2d: (32.8219800, -111.7853620)

1.4.8 SOOFIE

Company overview: ChampionX provides a wide range of emissions technologies tailored for the energy sector. Their portfolio includes Continuous Emissions Monitoring solutions, with systems, such as the Wireless Flare Monitoring, Emissions Monitoring, and Emission Control systems. These technologies are designed for real-time emissions tracking and control, ensuring compliance with environmental standards and enhancing operational efficiencies. Additionally, ChampionX's Artificial Lift Technologies segment offers systems and components, such as the SmartSpin Wireless Rod Rotator Sensor, Rod pump design & optimization software, and Progressing Cavity Pumping Systems, among others. These solutions aim to optimize production in the oil and gas sector while minimizing the environmental impact and upholding operational standards.[10]

Test equipment: The SOOFIE system consists of a network of pole-mounted metal-oxide semiconductor sensors, all adjusted for temperature and relative humidity. A Gill Windsonic 2D sonic anemometer is attached at approximately 7 feet off the ground on the SOOFIE sensor numbered "1". Each sensor continuously monitors methane and stores 1-minute averaged methane mixing ratios. The system then calculates a 15-minute-average site-level emission rate using various inputs, including methane mixing ratio, wind metrics, and a Gaussian plume transport model. The model doesn't compute an emission rate for wind speeds below 0.4 meters per second. Furthermore, the system only computes a site-level emission rate if the upwind surface influence function covers a source location listed in the site definition file.

Sensor locations:

- Unit 1: (32.82209039, -111.7862426)
- Unit 2: (32.82215808, -111.7859711)
- Unit 3: (32.82216873, -111.785754)
- Unit 4: (32.82217097, -111.7855359)
- Unit 5: (32.82213496, -111.7851938)
- Unit 6: (32.8218166, -111.7850969)
- Unit 7: (32.8215627, -111.7851534)
- Unit 8: (32.82128443, -111.7853871)
- Unit 9: (32.8212809, -111.785757)
- Unit 10: (32.8213059, -111.78614)
- Unit 11: (32.82164122, -111.786211)
- Unit 12: (32.82186578, -111.7862628)

1.4.9 Data submission

Table 3 presents the final data submission dates for various teams. The initial deadline for submitting the data was set for midnight on February 28 PT, 2023. However, due to logistical issues faced by continuous monitoring companies, the Stanford team decided to extend the deadline for all teams to March 31, 12:00 pm PT, 2023.

Two teams, Ecotec and SOOFIE, modified their submissions after the extended deadline due to timestamp issues. This is reflected in their later submission dates in the table.

Table 3: Data submission dates of all teams

Team name	Technology type	Data submission date
Ecotec	Point sensor network	2023-05-19
Project Canary		2023-03-31
Qube		2022-12-09
Sensirion		2023-03-31
SOOFIE		2023-06-13
Andium	Infrared camera	2023-04-03
Kuva		2023-03-31
Oiler		2023-03-31

1.4.10 Baker Huges - declined to participate

LUMEN Terrain, developed by Baker Hughes, is an IIOT system combining advanced sensor technology with innovative analytics. These all-weather sensors require no maintenance, are solar-powered, and operate independently from the grid, enhancing their reliability and cost-effectiveness. They continuously monitor methane emissions and H2S levels, along with environmental data such as temperature and wind conditions. The data collected is transmitted to a cloud-based system, accessible through an intuitive desktop application, displaying real-time and historical emission trends, anomalies, and potential leak areas. The system's deployment and management are straightforward, requiring minimal configuration from operators.[11] Baker Hughes declined to participate in the testing due to personnel limitations.

1.4.11 Honeywell Rebellion - declined to participate

Honeywell's Gas Cloud Imaging (GCI) system represents a state-of-the-art solution for industrial gas leak detection. Utilizing advanced infrared imaging technology, it provides real-time visualization of gas emissions, enhancing safety and compliance in industrial environments. This system claims to be beneficial in sectors handling hazardous gases, as it aids in quick identification and response to leaks, thereby ensuring operational safety and environmental sustainability.[12] Honeywell declined to participate in the testing due to personnel limitations.

1.4.12 Providence Photonics - declined to participate

Providence Photonics is a company specializing in advanced optical gas imaging (OGI) technology, addressing challenging environmental and safety problems in the industry. They offer solutions like leak quantification, leak survey validation, autonomous remote leak detection, and flare combustion efficiency monitoring. Their technologies utilize patented techniques, advanced computer vision, and state-of-the-art infrared imagers for various applications, particularly focusing on industrial gas leak detection and monitoring.[13] Providence did not respond after the Stanford team sent out invitations.

1.4.13 Cleanconnect.ai - declined to participate

CleanConnect.ai offers Autonomous365, a suite of AI-driven solutions aimed at hyper-automating critical infrastructure and energy operations. The suite includes tools for VOC gas monitoring and quantification, non-invasive tank monitoring, flame and smoke detection, and more. These solutions are designed to integrate with existing platforms or function as standalone systems, focusing on enhancing operational efficiency, safety, and environmental sustainability in the energy sector.[14] Cleanconnect.ai did not respond after the Stanford team sent out invitations.

1.5 Data processing for ground truth data and team reported events

In this section, we detail our data processing methods for both the ground truth data and the team-reported results. The primary challenge in data processing arose from the variable wind conditions observed during the two-month experimental period. To account for this, we incorporated daily meteorological data, which is presented in Table 4. We also developed a wind transport model to define Stanford releases, distinguishing between positive and negative events based on wind influence. Furthermore, we compare these Stanford-defined events with the events reported by the teams to assess discrepancies and align interpretations of the data. This comparative analysis helps in refining our understanding of the detection capabilities and limitations under varying environmental conditions.

1.5.1 Daily meteorological data

Table 4: Wind Speed Per Day

Date	**Wind Speed (m/s)**	**Date**	**Wind Speed (m/s)**	**Date**	**Wind Speed (m/s)**
2022-10-10	1.515	2022-10-28	2.269	2022-11-15	2.722
2022-10-11	2.602	2022-10-29	2.166	2022-11-16	2.890
2022-10-12	2.254	2022-10-30	2.755	2022-11-17	3.358
2022-10-13	2.306	2022-10-31	2.665	2022-11-18	2.398
2022-10-14	2.598	2022-11-01	3.094	2022-11-19	2.569
2022-10-15	NA	2022-11-02	4.095	2022-11-20	5.285
2022-10-16	2.052	2022-11-03	4.710	2022-11-21	2.197
2022-10-17	1.883	2022-11-04	1.501	2022-11-22	1.855
2022-10-18	5.013	2022-11-05	NA	2022-11-23	2.133
2022-10-19	4.682	2022-11-06	2.753	2022-11-24	3.273
2022-10-20	2.117	2022-11-07	3.135	2022-11-25	2.571
2022-10-21	2.655	2022-11-08	3.233	2022-11-26	2.829
2022-10-22	2.176	2022-11-09	5.685	2022-11-27	2.566
2022-10-23	6.329	2022-11-10	2.763	2022-11-28	2.740
2022-10-24	3.946	2022-11-11	2.523	2022-11-29	2.378
2022-10-25	2.221	2022-11-12	2.222	2022-11-30	2.617
2022-10-26	2.824	2022-11-13	3.704	-	-
2022-10-27	3.016	2022-11-14	2.419	-	-

1.5.2 Wind transport model

This section delves into the intricacies of understanding when non-zero methane release periods end, particularly for point sensor networks. The primary goal here is to ascertain when methane gas, once released, has entirely exited the defined experimental range, which can be counted as a non-zero event. This understanding is pivotal in characterizing the duration and cessation of a methane release event.

The model is grounded on a primary input: the distinction between zero and non-zero methane releases. By discerning the periods of actual methane release, the model can then gauge when this released methane drifts out of the twice the radius (or 163.8 meters from the release point) of the whole field site, thus marking the endpoint of the release period. Notably, camera-based systems are excluded from this model due to the nature of technology.

1. **Experimental range definition**: The experimental range, r, is set as 1, 2, or 4 times the radius of the smallest circumscribed circle within the experimental area. We've opted for twice the radius to ensure that point sensor networks can unambiguously detect when methane gas has entirely exited the defined range. Sensitivity analyses are performed for one and four times the radius to provide a comprehensive understanding, shown in S2.

2. **Calculate wind speed component**: For each non-zero release period, with s_i as the start time and e_i as the end time, calculate the total drift of methane gas up to the beginning of the next non-zero release period. This is done for each second t within this span, using U_t and V_t as drift metrics:

$$U_t = \sum_{s_i \leq t' \leq t} u_{t'} \tag{1}$$

$$V_t = \sum_{s_i \leq t' \leq t} v_{t'} \tag{2}$$

   Here, $u_{t'}$ and $v_{t'}$ represent the wind speed components in the east-west and north-south directions, respectively, at time t.

3. **End time update**: If a specific second $\hat{t}$ exists where the minimum drift distance d_t from s_i to e_i for all methane gas up to $\hat{t}$ is at least r, then $\hat{t}$ marks when all methane from the non-zero period has moved beyond the experimental range. As a result, e_i is updated to $\hat{t}$, as illustrated in figure 3. If the methane doesn't exit the range, the non-zero period is combined with the next one for further analysis, meaning s_{i+1} is adjusted to s_i.

The three steps are illustrated in figure 3. In summary, the goal is to determine when the gas released during a specific period has completely left the defined area. If this can be ascertained, that time is considered the end time. If not, due to factors such as calm winds or unpredictable drifts, the release period is considered to extend to the beginning of the subsequent release, effectively merging the events.

1.5.3 Data processing for Stanford-defined events.

The workflow for Stanford-defined events is depicted in figure 4. Both point sensor networks and camera-based technologies reported the start and end times for emission events. For actual release event alignment, it's imperative to define the events to synchronize with what each continuous monitoring solution reported. To align with these reports, we begin by gathering raw readings from wind and gas flow meters. This data is then refined by filling in missing values and adjusting for any gaps. Using the methane release rate dataset, we identify periods of gas releases and adjust boundaries based on wind transport models. This helps determine gas clearance periods, ensuring point sensor network events match with actual emissions detected on-site. Furthermore, data from internal tests and short-duration events are excluded for accuracy. The final process delivers two distinct Stanford-defined datasets, one for cameras and another for point network sensors (marked

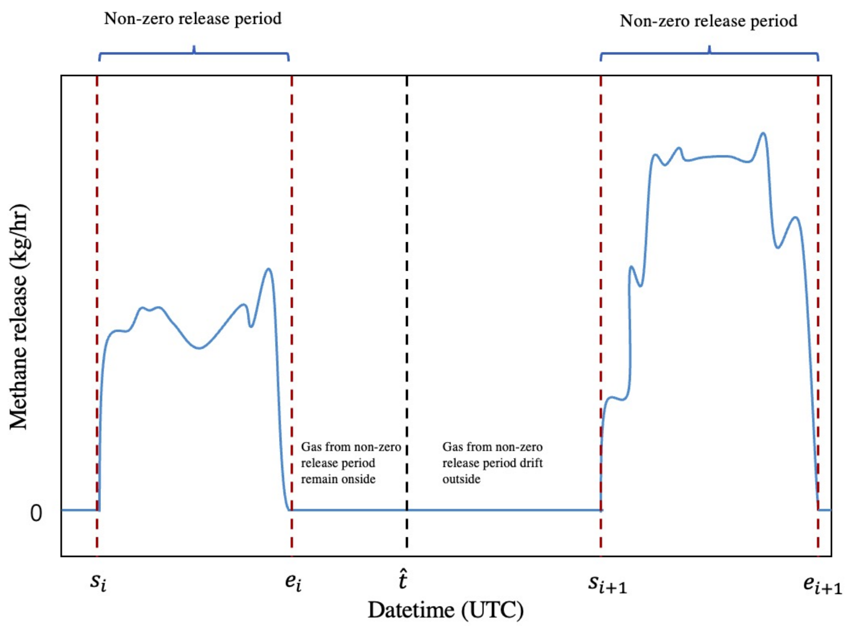

Fig 3: Wind transport model example. The graphical illustration of the methodology for tracking methane gas release and dispersion within a 2x radius of the experimental area. The graph displays two sets of methane releases controlled by the Stanford team. The rate of methane release, expressed in kilograms per hour (kg/hr), is plotted against a Coordinated Universal Time (UTC) timeline. Horizontal blue lines above each graph signify intervals of active methane emission, where the release is non-zero. Vertical dashed red lines, labeled s_i and e_i for the first event and s_{i+1} and e_{i+1} for the second event, determine the beginning and conclusion of these emission intervals. A vertical solid black line, denoted as $\hat{t}$, cuts through the graphs, highlighting a significant instant in time, such as when all methane from the non-zero release period has presumably moved beyond the 2x of the experimental area. Annotations within the graphs provide additional insights: "Gas from non-zero release period remains onside" suggests that the methane released remains within the set monitoring zone, while "Gas from non-zero release period drift outside" indicates that the methane has dispersed beyond the controlled area.

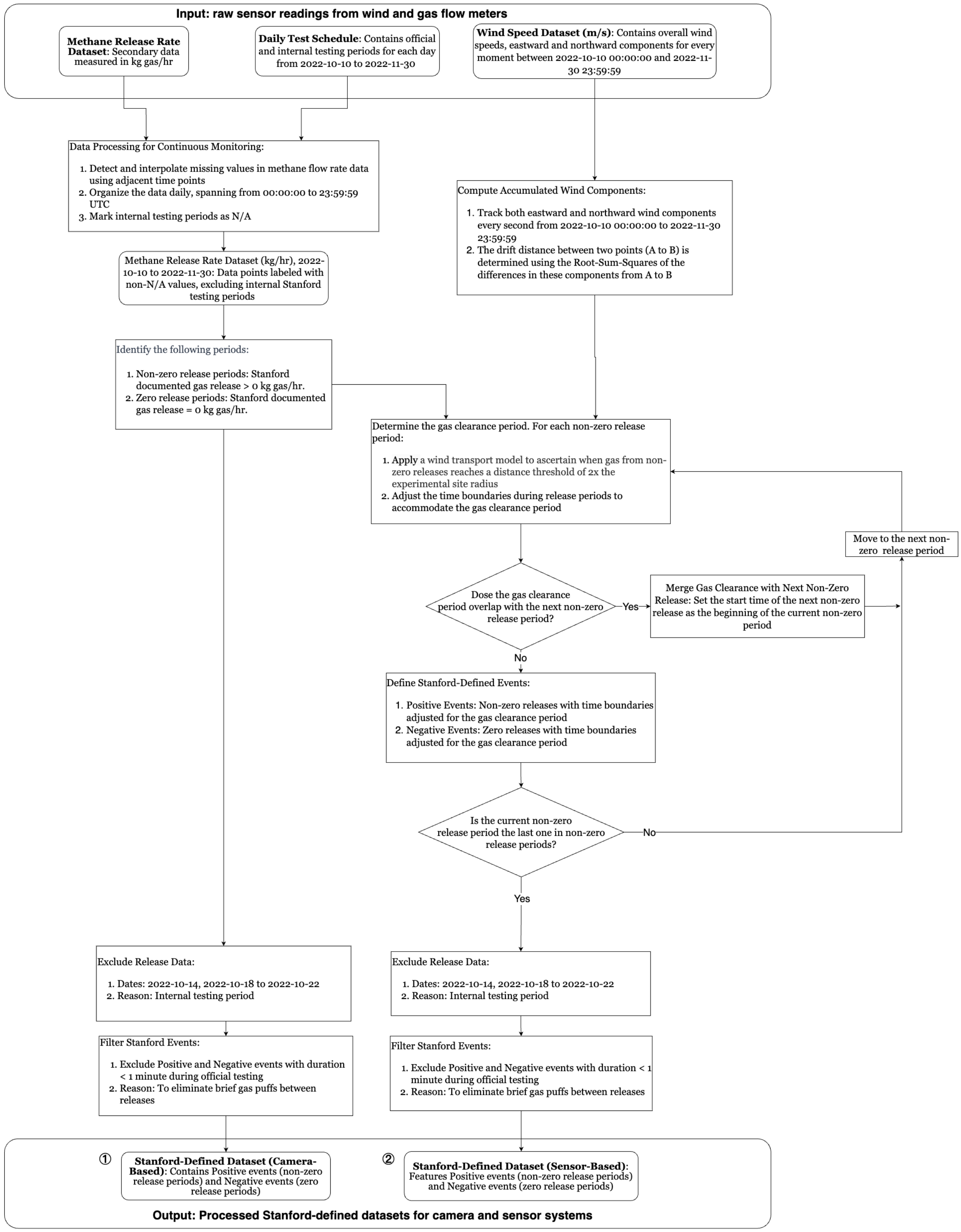

Fig 4: Stanford release data processing.

as 1 and 2 in figure 4), ensuring both align closely with reported data. These two datasets will be used as the input for evaluating the system's detection capability, as shown in figures 7, 8, and 9.

The figure 4 illustrates a systematic approach for processing raw sensor readings from wind and gas flow meters, along with methane release rate data, to produce datasets for camera and point network sensors. Initially, the raw data undergo interpolation for missing values and removal of internal testing intervals. The wind transport model is applied to identify non-zero and zero gas release periods and determines the gas clearance interval necessary to describe the release from non-zero intervals accurately. If a gas clearance period overlaps with a subsequent non-zero release period, the data are merged. Stanford-defined events, both positive and negative, are outlined with time boundaries adjusted for these periods. Finally, the events are filtered to include only those with a significant duration and to estimate transitional patterns between events, resulting in two refined datasets — one for camera-based and one for sensor-based monitoring systems — that catalog positive and negative methane emission events with associated time duration.

1.5.4 Data processing for team-defined events.

Figure 5 outlines how we process team-reported methane data. Teams that either only report methane detection events or provide specific release rates are indicated in the flow chart. SOOFIE uses a 15-minute average for release rates. Kuva, Oiler, and SOOFIE have offline periods attributable to system disconnections and homing errors; these periods are subsequently removed. Full raw reports from each team can be found on our Github. Unreported periods were interpreted as non-detections, equivalent to 0 kg/hr. The events are then categorized based on positive (emission period), negative (non-emission period), and N/A. They're matched with the team's submitted "Online Report Dates" to keep the data consistent. Any events that don't overlap with the provided dates are filtered out. The result is the "team-defined events Dataset" (marked as point 3 in figure 5). This dataset paves the way for the system performance evaluations in Figures 7, 8, and 9.

The workflow proceeds from top to bottom, starting with the collection of raw methane data from all continuous monitoring solutions. The data collected is organized by each team, which documents specific release event dates to track emissions; any unreported emissions are designated as zero-release periods. An event is categorized as positive when methane release rates exceed 0 kg/hr, as negative when rates are at 0 kg/hr, and marked as N/A when the rates are not available. Following this categorization, the data for each source is filtered with respect to the official report periods to ensure that there is no overlap with the system's offline periods. Any internal testing periods are excluded during this filtering process. The refined data is then compiled into a team-defined event dataset, segregated into positive, negative, and N/A events. This careful processing yields an organized output of team-defined datasets for camera and point sensor network systems.

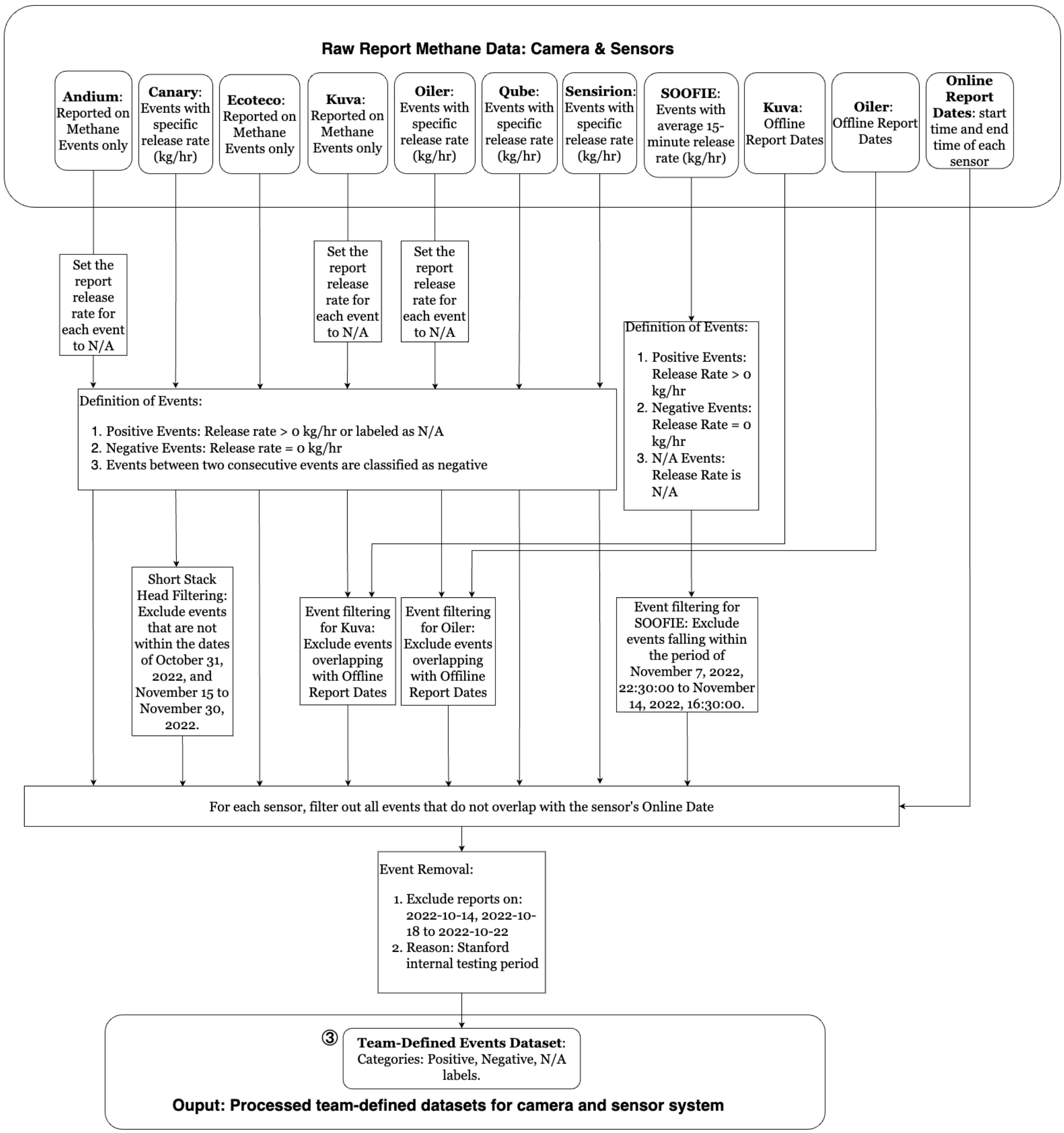

Fig 5: Team data processing.

1.6 Event matching and overlap criterion

The objective after processing both Stanford-defined and team-defined events is to correlate and classify them according to distinct standards. One key criterion is that any Stanford-defined events that overlap by over 50% with "N/A" (indicative of missing or not applicable data) were omitted from the analysis. The intricacies of this data processing can be better understood by referring to figures 7, 8, and 9. Specific classification rules are shown from table 5 to table 7.

1.6.1 Detection performance classification rules:

There are 2 distinct sets of rules for evaluating systems: time-based evaluation and event-based evaluation. Within event-based evaluation, there are two rules for classifying events: Stanford-defined events and team-defined events.

1.6.1.1 Stanford-defined events: Table 5 provides a systematic approach for categorizing Stanford-defined emission events by evaluating their intersections with Team-recognized events. This comparison answers the pivotal question: "When there is a release of gas onsite, is the continuous monitoring solution effectively identifying the emission?" The criteria within the table aid in drawing clear distinctions between different scenarios of overlap, shedding light on the monitor's precision and response in emission detection.

Table 5: Criteria for classifying Stanford-defined events based on overlap with team-defined events

Stanford-defined event	Matched team-defined events	Classification
Positive	Overlap $\geq$ 10% with all Positive Events	TP
Positive	Overlap $>$ 90% with all Negative Events	FN
Negative	Overlap $\geq$ 10% with all Positive Events	FP
Negative	Overlap $>$ 90% with all Negative Events	TN

1.6.1.2 Team-defined events: Table 6 establishes a method for categorizing team-defined emission events by comparing their overlaps with Stanford's recognized events. This comparison assesses the central query: "When the system detects an emission event, is there an actual release of gas onsite?" The criteria within the table serve to differentiate between various overlap scenarios, offering insights into the accuracy of the systems in emission detection.

Table 6: Criteria for classifying team-defined events based on overlap with Stanford-defined events

Team-defined event	Matched Stanford-defined events	Classification
Positive	Overlap $\geq$ 10% with all Positive Events	TP
Positive	Overlap $>$ 90% with all Negative Events	FP
Negative	Overlap $\geq$ 10% with all Positive Events	FN
Negative	Overlap $>$ 90% with all Negative Events	TN

396 **1.6.1.3 Time-based scenarios:** Table 7 provides a simplified interpretation of monitor performance in a time-based context. The approach is straightforward: at any specific moment, how precisely did the technology capture the status of the emission?

Table 7: Classification rules of time-based scenarios

True label[1]	Report label[2]	Classification
Positive	Positive	TP
Positive	Negative	FN
Negative	Positive	FP
Negative	Negative	TN

[1] True label: The labels for each second in the Stanford-defined scenario.
[2] Report label: The labels for each second in the Team-defined scenario.

399 *1.6.2 The example of classification rules:*

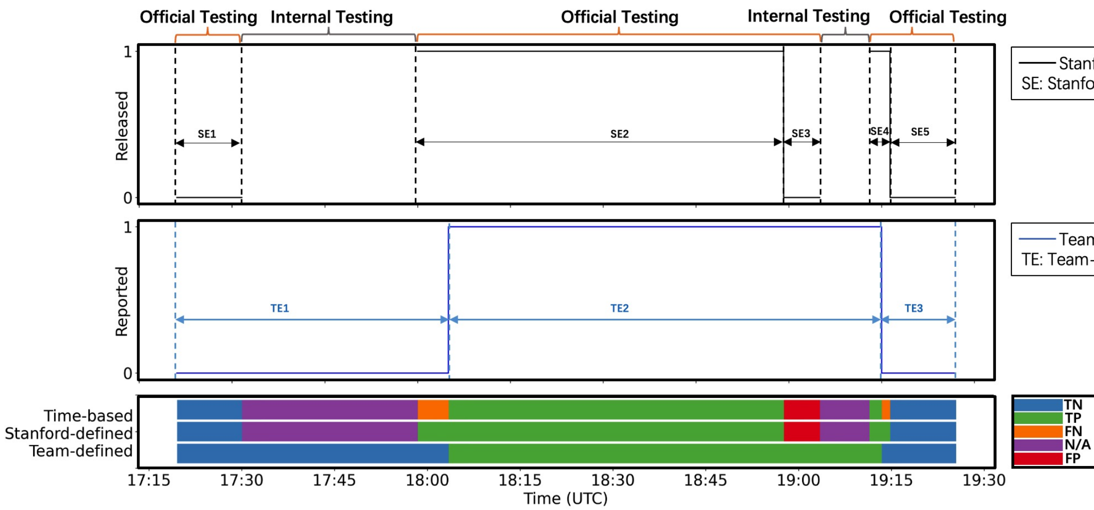

Fig 6: Examples of classification rules. This graph offers a detailed visual analysis of event reporting performance by different teams throughout a test day. It comprises three sections: The first section features two timelines—the Stanford-defined events marked with a thin black line and the Team-defined events with a thin blue line. These timelines are set against a background that alternates between "Official Testing" and "Internal Testing" periods, which are indicated by vertical dashed lines. The periods marked as N/A, corresponding to Internal Testing, are excluded from the evaluation. The second section, just below the timelines, displays a binary Y-axis which signifies the occurrence of an event from the Stanford or team perspective with upward spikes for each event detected. Events from the Stanford timeline are labeled "SE1" to "SE5," and from the team timeline as "TE1" to "TE3," with individual events marked by arrows and dashed lines. The third section is a color-coded timeline extending from 17:15 to 19:30, utilizing colored blocks to categorize events: True Negative (TN), True Positive (TP), False Negative (FN), Not Applicable (NA), and False Positive (FP). This linear representation offers a chronological sequence of event classifications. Overlap criteria are used to determine the relationships between Stanford-defined and team-defined events, while a time-based approach analyzes these relationships second by second, offering a granular view of the data. The detailed breakdown of this analysis is presented in Table 8, which provides a comprehensive understanding of event reporting accuracy and the effectiveness of the classification system in use.

400 Figure 6 presents event classifications for a specific testing day from one of the continu-
401 ous monitoring solutions. These classifications are based on the Stanford-defined, Team-defined,
402 and Time-based rules. Different colors, shown at the graph's bottom, mark these classifications.
403 Stanford-defined events are not continuous due to the filtering of internal testing periods. Any
404 overlapping team-reported events during these filtered periods are marked as N/A. On this day,
405 the upper part of the graph displays five Stanford-defined events (TE1-TE5), while the lower part
406 showcases three Team-defined events (RE1-RE3). Details about the labels assigned to these events
407 can be found in Table 8.

Table 8: Definition of each event on figure 6

Events	Label	Events	Label
TE1	Negative	TE2	Positive
TE3	Negative	TE4	Positive
TE5	Negative	RE1	Negative
RE2	Positive	RE3	Negative

In the Stanford-defined scenario, the classification results and overlap rate calculations for all events are summarized in Table 9. For example, TE1, a Negative event, overlaps only with RE1, a Negative event, resulting in a 0% Positive Overlap Rate (POR) and a 100% Negative Overlap Rate (NOR). Consequently, it's classified as TN.

Table 9: Stanford-defined events classification and overlap rates

Events	Matched positive Team-defined events	Matched negative Team-defined events	Positive overlap ratio (%)[1]	Negative overlap ratio (%)[2]	Classification
TE1	N/A	RE1	0	100	TN
TE2	RE2	N/A	100	0	TP
TE3	RE2	N/A	100	0	FP
TE4	N/A	RE3	0	100	FN
TE5	N/A	RE3	0	100	TN

[1] POR: calculated overlap ratio of all positive team-defined events
[2] NOR: calculated overlap ratio of all negative team-defined events

In the team-defined scenario, the overlap results and classifications for all events are detailed in Table 10. As an illustration, RE1, a Negative event that overlaps exclusively with TE1, has a POR of 0% and NOR of 100%, which results in a TN classification.

Table 10: Team-defined events classification and overlap rates

Events	Matched positive Stanford-defined events	Matched negative Stanford-defined events	Positive overlap ratio (%)[1]	Negative overlap ratio (%)[2]	Classification
RE1	N/A	TE1	0	100	TN
RE2	TE2	TE3	90	10	TP
RE3	TE4	TE5	18	82	FN

[1] POR: calculated overlap ratio of all positive team-defined events
[2] NOR: calculated overlap ratio of all negative team-defined events

For the time-based scenario, each second receives a "true label" (derived from Stanford-defined events) and a "report label" (derived from Team-defined events). If either of these labels is marked as N/A for a specific second, that second is not considered for classification. However, if both labels are present, the classification aligns with the time-based match rules.

1.7 Data processing for detection capability

This section provides a detailed insight into the data processing methods for evaluating the detection capabilities of systems in identifying emission events. It commences with the introduction of metrics used to evaluate the proficiency of systems in identifying Stanford-defined events and team-defined events. The metrics are essential in understanding the capability of the systems and their accuracy in identifying true emissions and non-emission periods.

Tables 11 and 12 serve to provide clear metric definitions. For the Stanford-defined events, the main focus is on how accurately the team-defined events recognize the Stanford-defined events. The metrics are described using the true positive rate (detection rate) and true negative rate (non-emission accuracy). This gives a clear indication of how efficient the system is at identifying actual emissions and non-emission periods.

For the team-defined events, the metrics shift the focus toward the reliability of the continuous monitoring reports. This is crucial in understanding the accuracy of team reports and how reliable they are in identifying actual Stanford-defined events. The metrics, in this case, are described using the positive predictive value (Reliability of identifications) and negative predictive value (Reliability of Non-emission identifications). This provides an understanding of the proportion of correct identifications by the teams in both emission and non-emission scenarios.

Following the introduction of metrics, the section details data processing workflows. Figures 7, 8, and 9) visualize these workflows clearly.

1.7.1 Metrics definition

Table 11 introduces the metrics used for the Stanford-defined confusion matrix. The primary question we seek to address with this matrix is: when a Stanford-defined event takes place, how accurately do the team-defined events recognize it?

Table 11: Metrics for Stanford-defined events

Metrics	Description
Detection rate (%)	Rate of correctly identifying actual emissions[1]
Non-emission accuracy (%)	Rate of correctly identifying no emission period[2]

[1] Detection rate: $\frac{TP}{TP+FN} * 100$
[2] Non-emission accuracy: $\frac{TN}{TN+FP} * 100$

Table 12 defines metrics for the team-defined confusion matrix. The inquiry we seek to address here is: when continuous monitoring reports an event, are they identified Stanford-defined events correctly?

Table 12: Metrics for team-defined events

Metrics	Description
Reliability of identifications (%)	Proportion of emission identifications that are accurate [1]
Reliability of non-emission identifications (%)	The proportion of non-emission identifications that are accurate[2]

[1] Reliability of identification: $\frac{TP}{TP+FP} * 100$
[2] Reliability of non-emission identifications: $\frac{TN}{TN+FN} * 100$

1.7.2 Data processing for Stanford-defined events-based evaluation.

This diagram 7 outlines the analytical process for event-based methane emission data, integrating outputs from team data processing (see Figure 5) and Stanford release data processing (see Figure 4) as foundational inputs. Initially, the flow chart addresses the categorization of processed data into positive, negative, and N/A (not available) event classifications derived from both team-defined and Stanford-defined sources, corresponding to the monitors' reported data, including the downtime periods. The analysis proceeds by seeking overlaps between the team-defined and Stanford-defined emission events. When an overlap occurs, the process involves calculating an overlap ratio by examining the duration of these simultaneous events. This ratio is critical as it influences whether a Stanford-defined event is considered a True Positive or False Negative based on set threshold levels. If there is no overlap, the analysis continues to the next Stanford-defined event. Each event ultimately receives a classification as True Positive, True Negative, or N/A, determined by its concurrence with a team-defined event. The final step of this flow chart is to derive two key metrics: the detection rate, which evaluates the frequency of correctly identified emission events, and non-emission accuracy, which assesses the correct identification of non-emission instances.

Figure 7 demonstrates the systematic approach in evaluating the detection capabilities of the systems using Stanford-defined events. The primary outcome is the detection rate and the non-emission accuracy, which will provide a clear understanding of how efficiently the continuous monitoring solutions can identify true emission events using the systems.

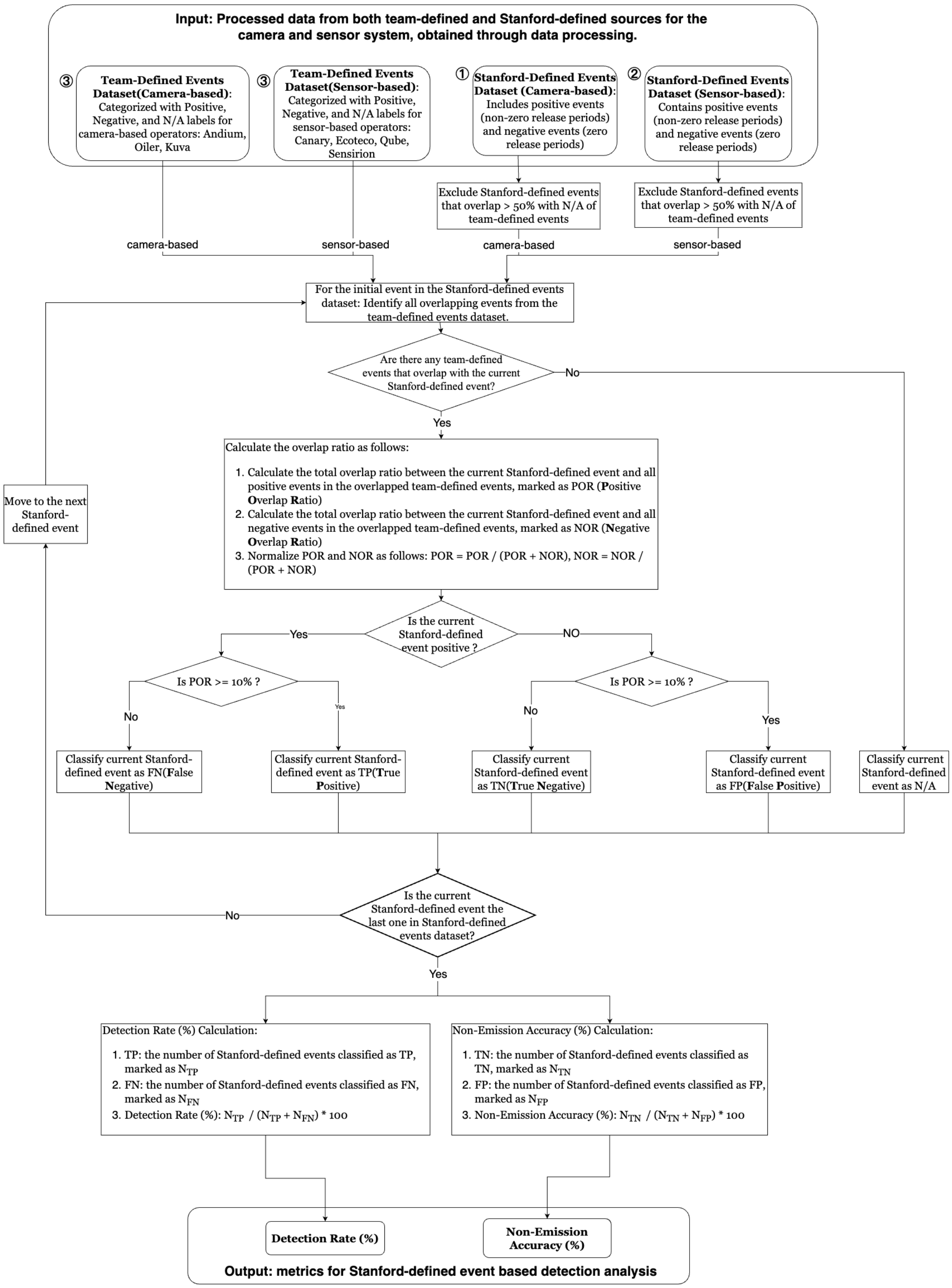

Fig 7: Stanford-defined events flow chart.

1.7.3 Data processing for team-defined events-based evaluation.

This flow chart 8 begins with integrating processed information from both team-defined and Stanford-defined datasets, which are associated with camera and point network sensors (refer to Figure 5 and Figure 4 for detailed data processing). The data is classified into three categories—positive, negative, or N/A (not applicable)—based on the release rates reported during both active monitoring and system downtime periods. Events that match across both datasets are marked as True Positives or False Negatives, based on an overlap ratio that must meet a specific threshold. If there's no match, the Stanford-defined event is reviewed further. The final classifications — True Positive, True Negative, or N/A — depend on whether Stanford-defined events align with team observations. The effectiveness of this method is measured by two main metrics: the rate of correctly identified emission events (reliability of identification) and the rate of correctly identified non-emission events (reliability of non-emission identification), essentially assessing the system's accuracy in monitoring methane emissions

Figure 8 flowchart shifts the focus towards the continuous monitoring solutions' perspective and evaluates the reliability of their reports. It elucidates the procedure to derive metrics for team-defined events, checking overlaps with Stanford-defined events. The outcome provides a clear understanding of the system's effectiveness in event recognition from the monitor's reported perspective.

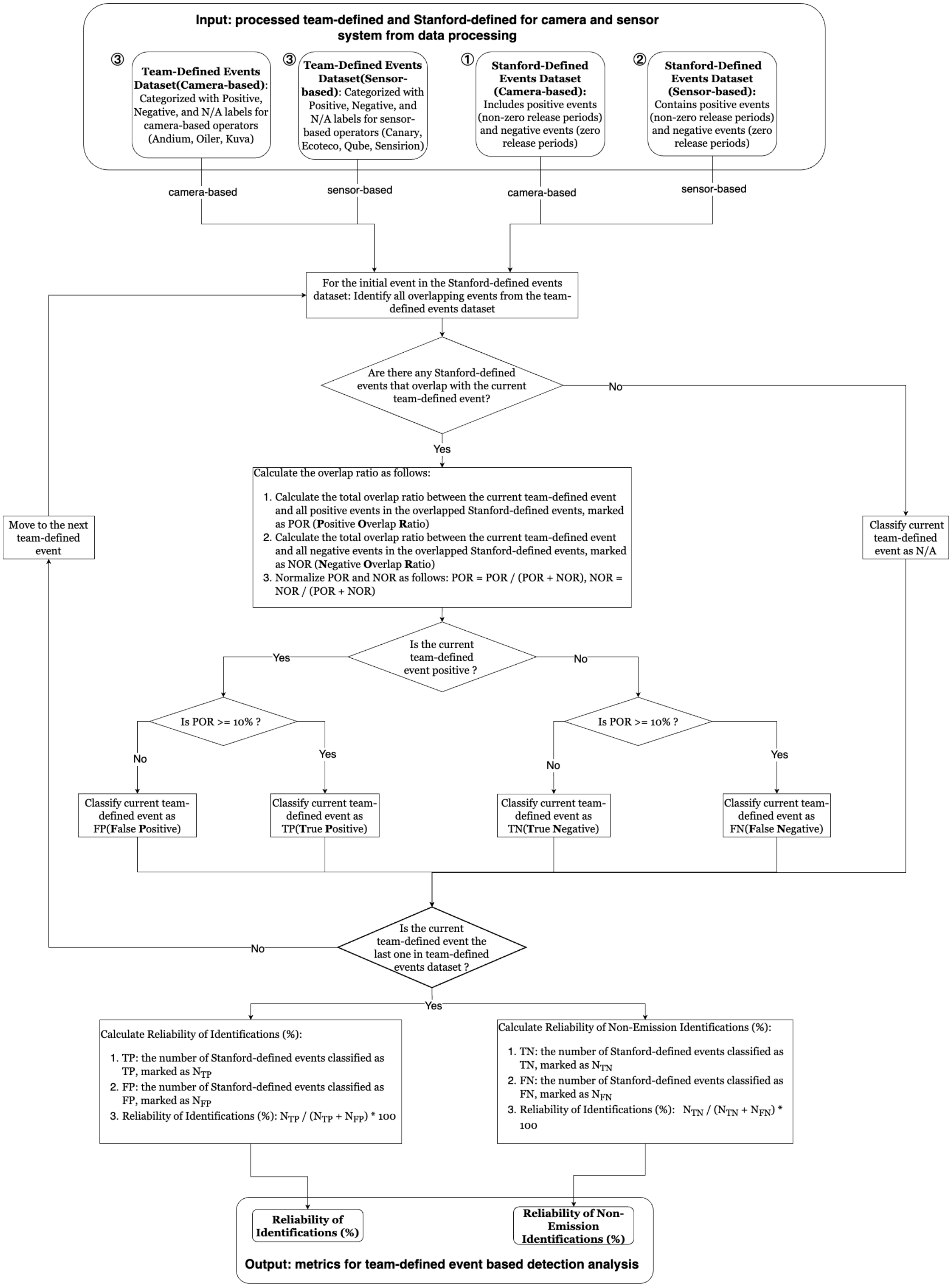

Fig 8: Team-defined events flow chart.

1.7.4 Data processing for time-based metric evaluation.

This chart 9 presents the workflow for comparing and validating methane emission events from team-defined and Stanford-defined data. The process begins by categorizing each event from these datasets into one of three types: positive, negative, or N/A (not applicable), considering the specific operational period. Each event from the team-defined dataset is then matched against the Stanford-defined dataset to check for temporal overlap on a second bases. Events are validated if they coincide in time; the Stanford-defined event is classified as True Positive (TP) if it overlaps with a team-defined event, or True Negative (TN) if it does not. The flow progresses iteratively through each event, ultimately calculating key performance metrics: True negative rates, true positive rates, false positive rates, false negative rates, accuracy, and precision.

Figure 9 presents a time-based approach to validate team-reported emission events, drawing on data from Figures 4 and 5. Using data from both camera and sensor systems, the method categorizes team-defined events into positives, negatives, and N/A. Categorizing the events on a second-by-second basis and subsequently evaluating the time-based detection metrics, provides insight into how accurately a particular technology reports the emission status over time.

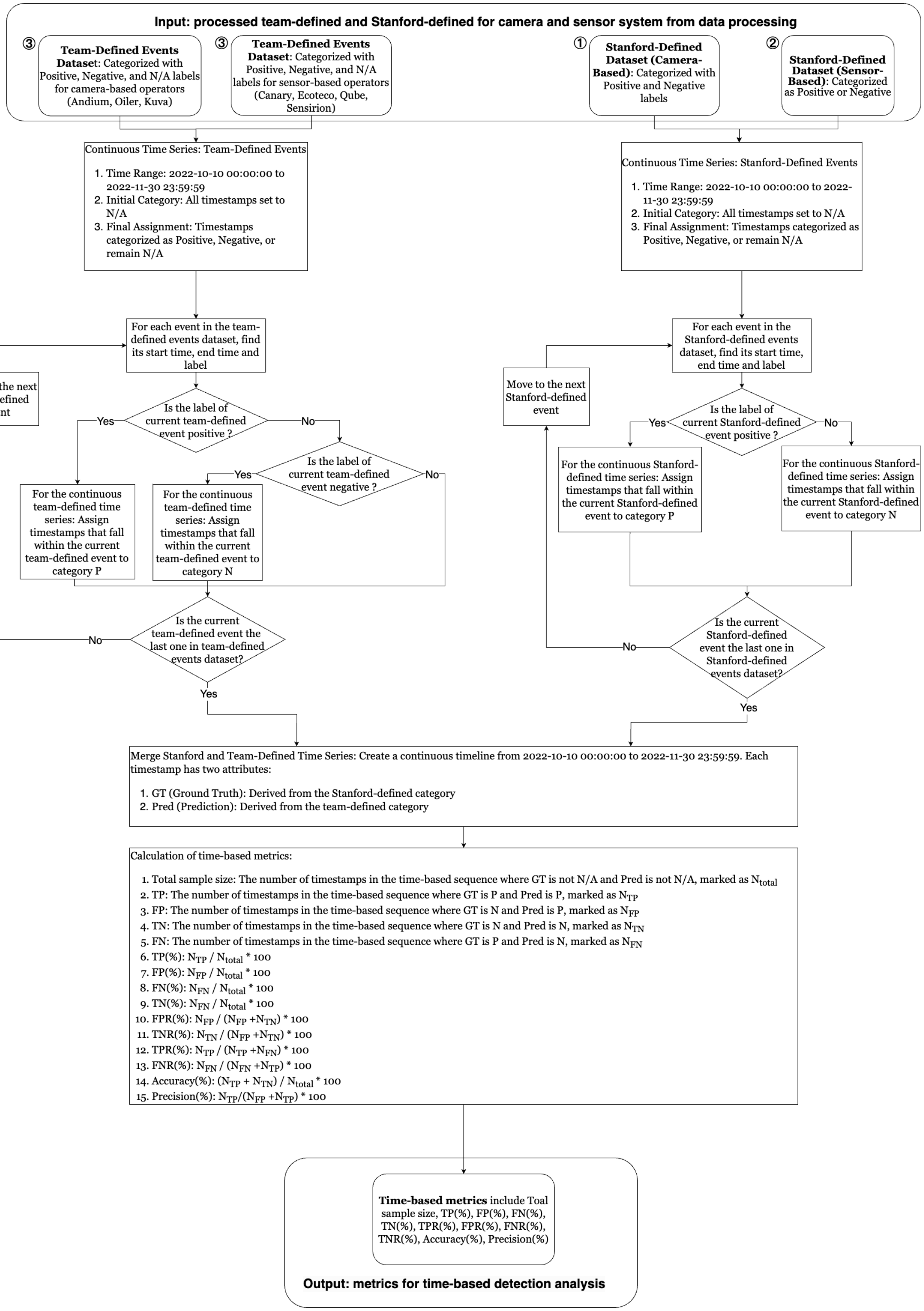

Fig 9: Time-based flow chart.

S2 Supplementary Results

2.1 Supplementary detection results

2.1.1 Event-based detection result

Figure 10 shows a collection of bar charts for different sensor technologies, comparing the percentage of detection events to the duration of gas releases during the experiment. Table 14 presents the event-based detection results under three radius thresholds of the wind transport models for four point sensor networks. Camera-based technology did not apply the wind-transport model due to the nature of the technology type. An analysis of the data reveals minimal variations in metrics as the threshold shifts from 1x to 4x for each model. The consistency across these metrics, regardless of the model or threshold applied, suggests that the event-based result of each system remains stable across different threshold values within the parameters of this study.

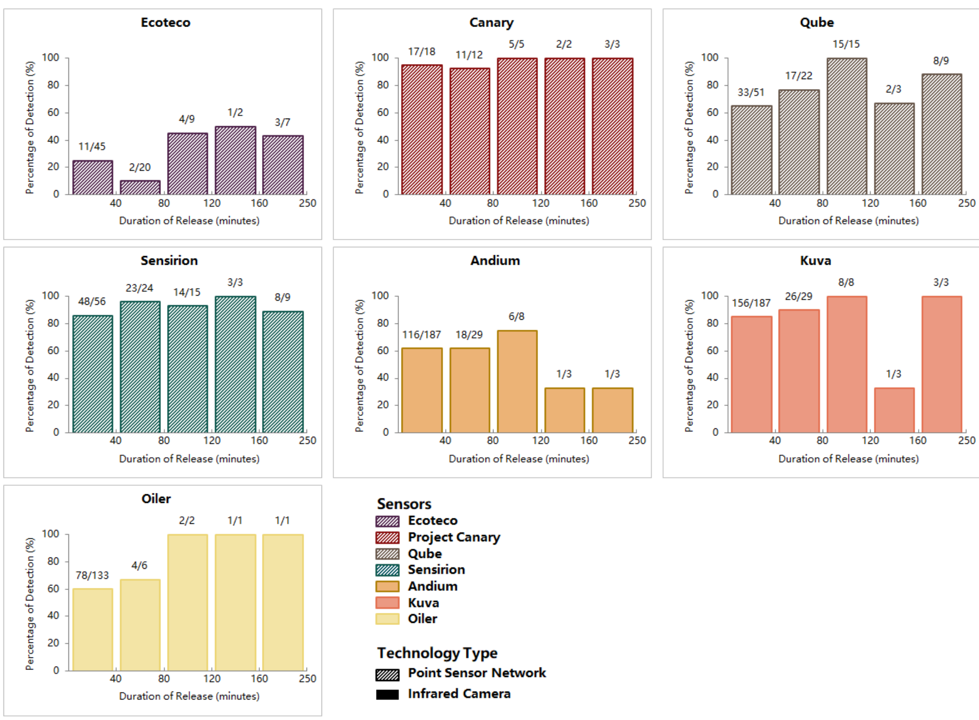

Fig 10: Team probability of detection affected by the duration of methane release. The bar charts display the efficacy of various sensor technologies in detecting gas releases over different durations. Each bar corresponds to a category of release duration, with the percentage of successful detections plotted on the y-axis. The higher the bar, the greater the detection rate for that time interval. The numbers above the bars indicate the actual count of detections versus the total possible for that duration, giving a precise success ratio for each interval. The color and pattern of the bars are keyed to the sensor technology types, allowing for comparison across technologies.

Sensor technologies, such as Canary and Sensirion, perform better at detecting emissions over some durations than others. Continuous monitoring solutions show various success rates depending on the duration of the gas release. This visual representation helps identify which technologies might be more suitable for quick leaks versus sustained releases. However, long events make up a small portion of the overall event sample, and thus additional testing is required to further explore this relationship.

Table 13 presents the comprehensive event-based evaluation result of each continuous monitoring solutions. For detail graphs, refer to figure 4 in the main paper.

Table 13: Results of event-based detection for each system

Team	**Technology type**	**Stanford perspective**		**Team perspective**	
		Detection rate (%)[1]	**Non-emission accuracy (%)**[2]	**Reliability of identifications(%)**[3]	**Reliability of non-emission identifications (%)**[4]
Ecotec	Point sensor network	25.61	95.15	73.45	29.37
Project Canary		95.00	49.06	90.91	96.15
Qube		75.00	74.24	86.21	47.90
Sensirion		89.72	54.11	84.21	90.67
Andium	Infrared camera	62.56	87.25	94.62	60.00
Kuva		91.94	73.64	95.74	43.48
Oiler		69.92	92.86	97.22	28.00

[1] Detection rate (%): This is called a true positive rate or sensitivity, calculated as $\frac{TP}{TP+FN} * 100$. This is the percentage of correctly identified Stanford emissions

[2] Non-emission accuracy(%): This is called a true negative rate or specificity, calculated as $\frac{TN}{TN+FP} * 100$. Non-emission accuracy refers to the percentage of correctly identified Stanford periods of non-emissions

[3] Reliability of identifications(%): This is called a positive predictive value or precision, calculated as $\frac{TP}{TP+FP} * 100$. This refers to the percentage of continuous monitoring teams that reported emissions that are correct.

[4] Reliability of non-emission identifications (%): This is called a negative predictive value, calculated as $\frac{TN}{TN+FN} * 100$. This refers to the percentage of continuous monitoring teams that reported non-emission periods that are correct.

Table 14: Event-based performance in response to adjustments in wind transport model radius threshold

Point sensor networks	Radius threshold	Number of Stanford-defined events	Number of team-defined events	Stanford perspective		Team perspective	
				Detection rate (%)	Non-emission accuracy (%)	Reliability of identifications (%)	Reliability of non-emission identifications (%)
Ecotec	1	193	1039	27.27	94.29	73.25	30.3
	2	185	1039	25.61	95.15	73.45	29.37
	4	173	1041	25.33	96.94	74.5	28.39
Project Canary	1	98	37	95.35	47.27	90.91	96.15
	2	93	37	95.0	49.06	90.91	96.15
	4	89	37	94.74	50.98	90.91	96.15
Qube	1	248	206	72.73	71.74	86.21	47.9
	2	232	206	75.0	74.24	86.21	47.9
	4	218	206	74.73	76.38	87.36	47.9
Sensirion	1	269	113	90.6	51.97	84.21	90.67
	2	253	113	89.72	54.11	84.21	90.67
	4	238	113	88.78	55.0	84.21	86.67

We conducted analysis to evaluate how the magnitude of the emission rate influences the detection probability of various continuous monitoring solutions, with the results displayed in figure 11. This analysis is critical for understanding each system's responsiveness to different levels of methane emissions, which in turn informs their suitability for applications requiring early detection and precise measurement. We found that certain teams have shown clear improvement in detection as the magnitude of rates increases, while others do not.

Some technologies maintain a relatively stable detection rate across different release rates, suggesting robustness in detecting both low and high emissions. Other technologies show increasing percentage of detection rate as release rates increase. These suggest varying degrees of sensitivity and effectiveness among the different technologies in response to the magnitude of methane emissions. The graph suggests complexity in detection performance, emphasizing the need to consider each technology on a case-by-case basis when evaluating its efficacy for different magnitudes of methane emissions.

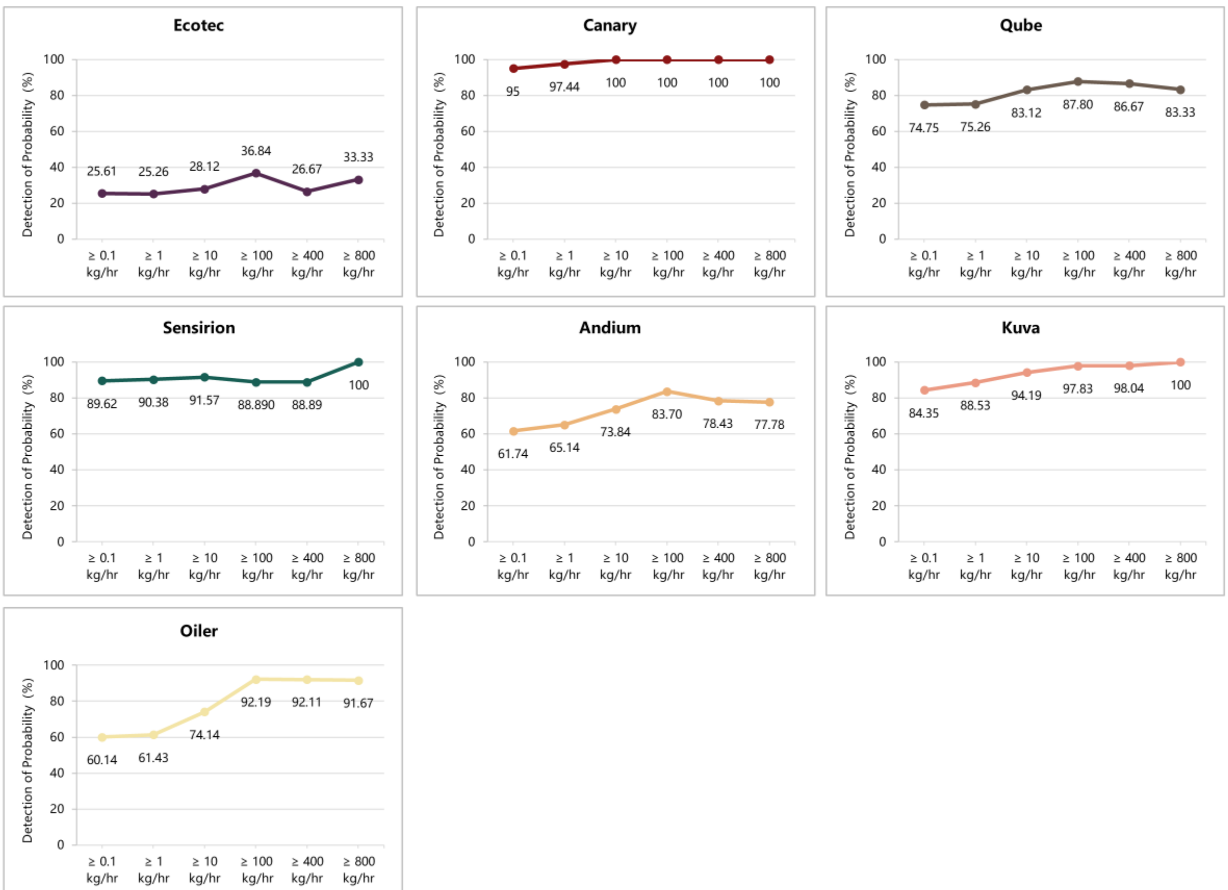

Fig 11: Probability of detection v.s magnitude of emission rates. The set of line graphs represent a different continuous monitoring solution's detection probability across various average methane release rates. The X-axis shows the increasing average release rates of methane, starting from greater and equal to 0.1 kg/hr and moving to higher thresholds up to 800 kg/hr. Y-axis represents the detection probability percentage for each technology. Each graph line corresponds to a particular sensor technology and is plotted with points at each average release rate category. The lines connect these points, illustrating the change in detection probability as the release rate increases.

2.1.2 Sensitivity analysis

Both figure 12 and table 15 details the event-based detection results of various systems with the overlap criteria adjusted from 10% to 50%. This shift in assessment criteria is crucial to note, especially when contrasted with the original 10-90% overlap results outlined in Table 6 and the main paper. The new criteria require system data to match more closely with the duration of Stanford-defined events for accurate classification as true positives, thereby presenting a more rigorous test of the systems' ability to monitor emission events accurately and consistently. Moreover, the change in the false positive threshold from 90% to 50% lessens the stringency, potentially leading to a decrease in the number of false positives identified by systems.

Table 15: Event-based detection performance of systems at 50% overlap rate adjustment

Team	**Technology type**	**Stanford perspective**		**Team perspective**	
		Detection rate (%)[1]	**Non-emission accuracy (%)**[2]	**Reliability of identifications(%)**[3]	**Reliability of non-emission identifications (%)**[4]
Ecotec	Point sensor network	1.22	100.00	73.25	33.08
Project Canary		95.00	50.94	90.91	100.00
Qube		49.00	78.03	86.21	60.50
Sensirion		86.92	57.53	76.32	96.00
Andium	Infrared camera	58.59	93.29	94.62	69.23
Kuva		90.05	78.18	95.04	51.63
Oiler		57.72	96.43	97.22	34.40

[1] Detection rate (%): $\frac{TP}{TP+FN} * 100$
[2] Non-emission accuracy (%): $\frac{TN}{TN+FP} * 100$
[3] Reliability of identifications (%): $\frac{TP}{TP+FP} * 100$
[4] Reliability of non-emission identifications (%): $\frac{TN}{TN+FN} * 100$

In light of these changes, the performance of systems varies considerably. Continuous monitoring solutions, such as Andium, Ecotec, Oiler, and Qube show detection rates falling below 60%. This downturn suggests difficulties these systems face in maintaining accurate alerts that reflect the start and end times of emission events. On the other hand, Kuva, Project Canary, and Sensirion demonstrate strong performance despite the tighter criteria, indicating their technologies are better equipped for detailed, continuous monitoring and for effectively assessing the duration of emission events. This divergence in performance becomes more pronounced when comparing camera-based solutions to point sensor networks, highlighting the differing responses to the new criteria.

The revised criteria, leading to fewer instances being classified as false positives, are expected to increase the non-emission accuracy and reliability of identifications. This improvement suggests an enhancement in the overall accuracy and reliability of the systems. Such shifts in performance benchmarks highlight the ongoing need for innovation and adaptation in continuous monitoring technology, emphasizing its critical role in effective environmental monitoring.

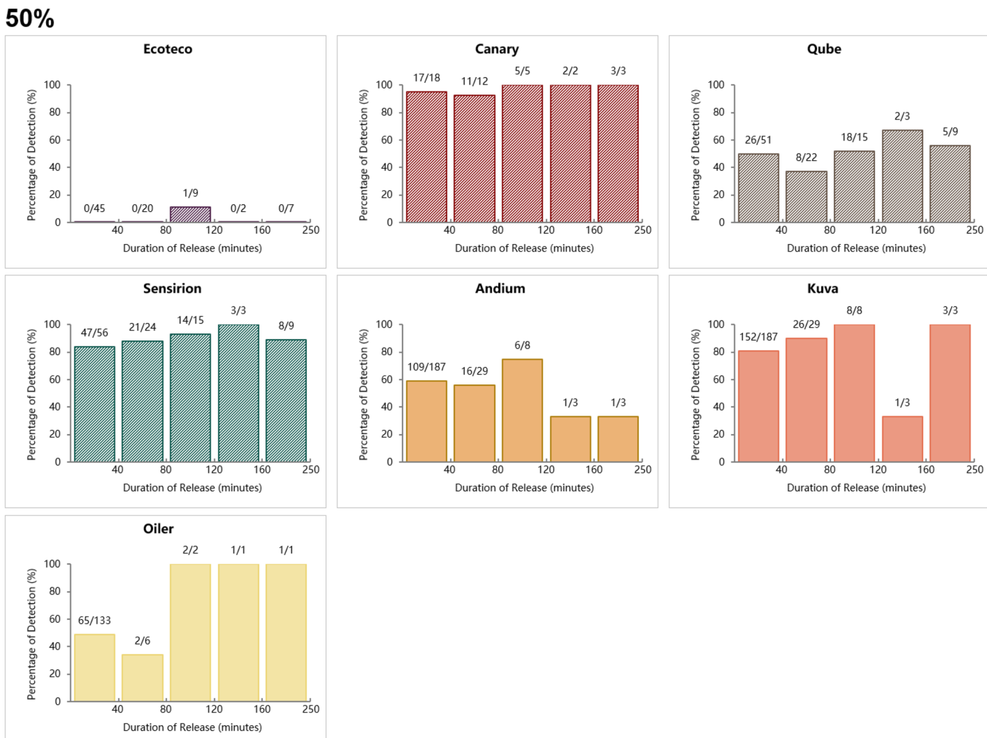

Fig 12: Team probability of detection (50% overlap ratio) affected by duration of methane release. The bar charts display the efficacy of various sensor technologies in detecting gas releases over different durations. Each bar corresponds to a category of release duration, with the percentage of successful detections plotted on the y-axis. The higher the bar, the greater the detection rate for that time interval. The numbers above the bars indicate the actual count of detections versus the total possible for that duration, giving a precise success ratio for each interval. The color and pattern of the bars are keyed to the sensor technology types, allowing for comparison across technologies.

2.1.3 Time-based evaluation data

We presented additional analyses conducted on the time-based detection results. We investigated how average wind speed affects the true positive rates for each team, as illustrated in Figure 13. This analysis provides insights into how wind conditions influence sensor performance. Additionally, we evaluated each sensor's performance by analyzing second-by-second data samples collected during their online periods and deployment phases, detailed in Table 16. Furthermore, we performed a sensitivity analysis on the adjustment of the experimental range used in our wind transport model. This analysis helps in understanding the robustness of our model under different wind conditions and informs potential adjustments for future experiments.

2.1.4 True Positive Rate vs. Average Wind Speed

Figure 13 shows multiple dots for each sensor type, indicating that each sensor's true positive rate was measured at different average wind speeds to assess performance under varying meteorological conditions.

The impact of wind speed on the true positive rate varies across the different sensors. For some sensors, the true positive rate remains fairly constant as the wind speed increases. However, some test participants, such as Ecotec, show decreasing performance with increasing wind speed, while others, like Oiler, demonstrate improved performance as wind speeds increase.

Wind speed can considerably affect certain sensor efficacy. Future studies are essential, particularly those that examine high-volume releases under variable wind conditions. Such research could offer more definitive answers to the nuanced impacts of wind speed on emissions detection, especially concerning larger emission events.

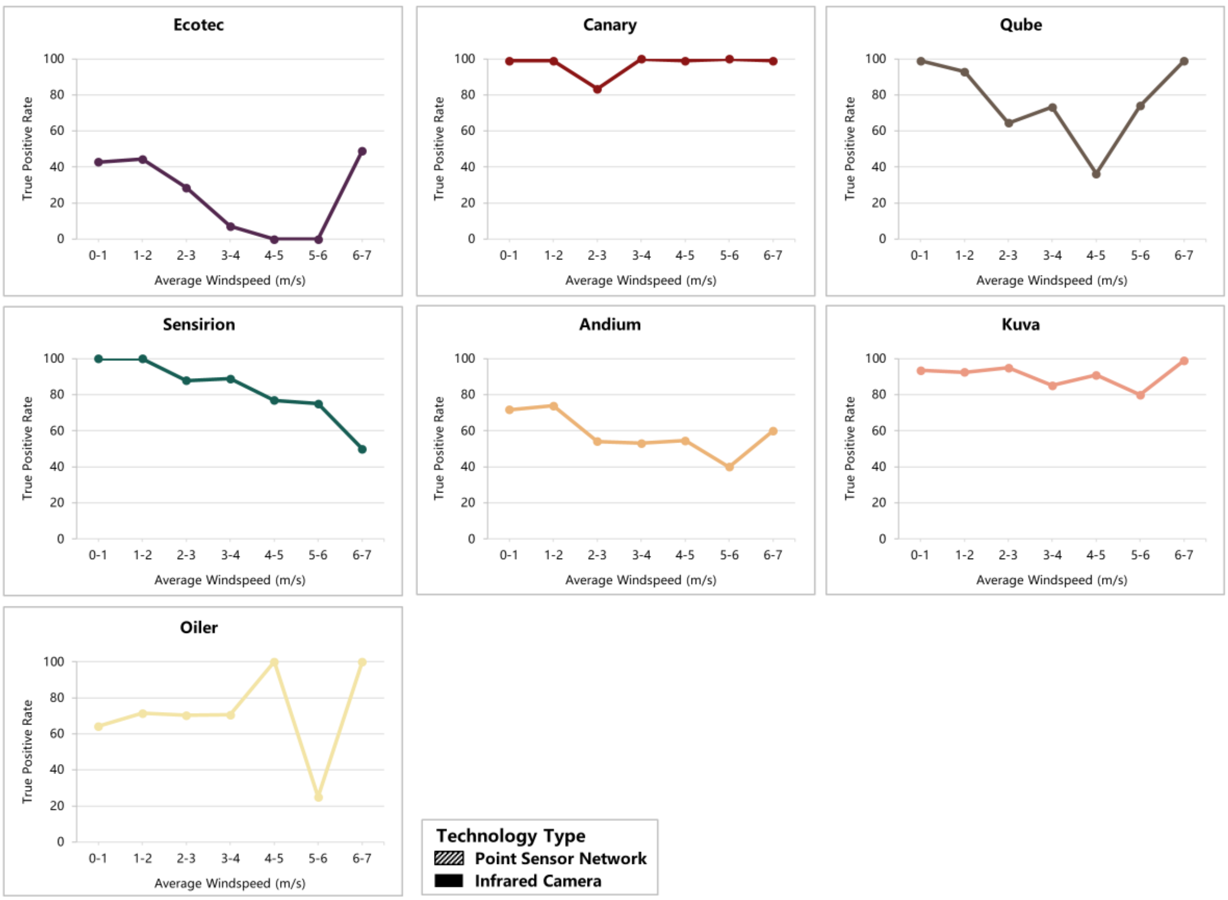

Fig 13: True Positive Rate vs. Average Wind Speed. The graph plots the relationship between the true positive detection rate of various sensors and the average wind speed during detection times. The true positive rate is measured as a percentage and is displayed on the y-axis, which ranges from 0 to 100%. The average wind speed, measured in meters per second (m/s), is shown on the x-axis, which is divided into ranges (0-1, 1-2, and so on up to 6-7 m/s). Each colored dot represents a different sensor, as indicated by the legend on the right side of the graph.

2.1.5 Team Time-based evaluation data

Table 16 emphasizes that the release seconds and total evaluated seconds account for the operational periods of the sensors, thereby reflecting the conditions under which the teams' equipment was tested. The release percentage, as defined in the footnote, indicates each team's sensor capacity for detecting releases under optimal conditions. For a comprehensive analysis of the actual true positive detections achieved by each team's sensors, the reader is referred to Figure 2 in the main paper. This figure provides a visualization of the actual detection performance, illustrating how frequently each team's sensors correctly identified the presence of gas releases during the experiment. This complements the information presented in the table by showcasing the realized detection capabilities as opposed to the maximum potential denoted by the release percentage.

Table 16: Sensor Evaluation Data

Team Name	**Technology Type**	**Release Seconds (s)**[1]	**Total Evaluated Seconds(s)**[2]	**Release Percentage (%)**[3]
Ecoteco	Point sensor network	267,250	2,639,159	10.13
Project Canary		144,881	1,354,747	10.69
Qube		358,252	3,147,247	11.38
Sensirion		371,678	3,738,986	9.94
SOOFIE		212,017	2,528,490	8.39
Andium	Infrared camera	332,823	3,128,980	10.64
Kuva		324,576	914,142	35.51
Oiler		129,944	1,081,843	12.01

[1] The "Release Seconds" refers to the cumulative duration, measured in seconds, during which the Stanford team actively released gases as part of the detection trials. This measure varies as it is contingent upon the periods when the participating teams were both deployed in the field and their equipment was operational and online. Hence, the evaluation of the release seconds is specific to those intervals when teams were capable of detecting emissions, ensuring that our analysis accurately reflects the real-world performance of the sensors under test conditions.

[2] The "Total Evaluated Seconds" encompasses the entire duration for which each team's detection capabilities were assessed. This includes both 'release seconds'—the time when gas was actively being released and could potentially be detected—and 'non-release seconds'—when there was no gas release. The total evaluated seconds thus constitute the sum of these two measures. It is important to note that this total varies between teams due to the differences in the duration of each team's equipment being operational and online throughout the experiment. The variation in online periods across teams results in differing amounts of data for analysis, reflecting the real-time operational conditions each team experienced during the trials.

[3] The "Release Percentage" represents the maximum proportion of true positive detections that a team could theoretically achieve during the periods when the Stanford experiment actively released gases. This metric indicates the upper limit of a team's detection capability under the controlled conditions of the experiment, assuming perfect sensor performance and no false negatives. Essentially, it quantifies the best-case scenario for each team's sensor technology in recognizing and responding to the gas release events orchestrated by the experiment.

2.1.6 Time-based detection result

Table 17 shows the tabular form of figure 3 in the main paper of all continuous monitoring solution time-based detection results. All formulas and definition of each metric is defined in the footnote.

Table 18 showcases the sensitivity analysis results for four point sensor network models when subjected to different threshold values. Camera-based technology did not apply the wind-transport model due to the nature of the technology type. The columns represent different metrics of the

Table 17: Results of time-based detection for each system

Team	Technology type	Times %				Rate while emitting		Rate while not emitting		Efficacy of system detection	
		TP(%)[1]	FP(%)[2]	TN(%)[3]	FN(%)[4]	TPR(%)[5]	FPR(%)[6]	TNR(%)[7]	FNR(%)[8]	Accuracy(%)[9]	Precision(%)[10]
Ecotec	Point sensor network	0.98	0.84	89.03	9.14	9.71	0.94	99.06	90.29	90.02	53.89
Project Canary		10.29	1.42	87.89	0.41	96.21	1.59	98.41	3.79	98.18	87.87
Qube		5.98	0.64	87.97	5.40	52.57	0.73	99.27	47.43	93.96	90.29
Sensirion		8.92	2.46	87.60	1.02	89.77	2.74	97.26	10.23	96.52	78.36
SOOFIE		7.23	7.96	83.66	1.16	86.21	8.69	91.31	13.79	90.88	47.60
Andium	Infrared camera	6.13	0.14	89.22	4.51	57.63	0.16	99.84	42.37	95.35	97.77
Kuva		29.25	0.99	63.50	6.25	82.38	1.53	98.47	17.62	92.76	96.73
Oiler		6.68	0.22	87.77	5.33	55.60	0.25	99.75	44.40	94.44	96.78

[1] True Positives(%): $\frac{TP}{TP+FP+TN+FN} * 100$, indicating the percentage of instances where the system correctly identifies the presence of emissions.
[2] False Positives(%): $\frac{FP}{TP+FP+TN+FN} * 100$, indicating the percentage of instances where the system incorrectly signals the presence of emissions when there are none.
[3] True Negatives(%): $\frac{TN}{TP+FP+TN+FN} * 100$, indicating the percentage of instances where the system correctly identifies the absence of emissions
[4] False Negatives(%): $\frac{FN}{TP+FP+TN+FN} * 100$, indicating the percentage of instances where the system fails to detect emissions when they are actually present.
[5] True Positive Rates(%): $\frac{TP}{TP+FN} * 100$, measuring the system's effectiveness in correctly identifying emissions relative to all actual emissions.
[6] False Positive Rates(%): $\frac{FP}{FP+TN} * 100$, measuring the percentage of the system incorrectly identifying emissions relative to all actual non-emissions.
[7] True Negative Rates(%): $\frac{TN}{FP+TN} * 100$, measuring the accuracy in identifying the absence of emissions relative to all actual non-emissions.
[8] False Negative Rates(%): $\frac{FN}{TP+FN} * 100$, measuring the rate at which the system misses detecting emissions relative to all actual emissions.
[9] Accuracy(%): $\frac{TP+TN}{TP+FP+TN+FN} * 100$, measuring the overall accuracy of the system in detecting both emissions and non-emissions.
[10] Precision(%): $\frac{TP}{TP+FP} * 100$, measuring the overall accuracy of the system when it detects emissions, out of all reported emissions.

models' efficiency, including True Positives (TP), False Positives (FP), True Negatives (TN), False Negatives (FN), and their corresponding rates.

Three threshold levels are considered for each wind-transport model: 1x, 2x, and 4x. An examination of the metrics across these radius thresholds indicates minor variations as the threshold values change. Despite the variation in thresholds and models, the performance metrics of the wind transport model show a notable consistency. This suggests that the time-based result of each point sensor network remains largely unaffected by the variations in threshold values within the scope of this study.

Table 18: Time-based performance in response to adjustments in wind transport model radius threshold

Point sensor networks	Threshold	Samples (s)	Times %				Rate while emitting		Rate while not emitting		Efficacy of system detection	
			TP (%)	FP (%)	FN (%)	TN (%)	TPR (%)	FPR (%)	FNR (%)	TNR (%)	Accuracy (%)	Precision (%)
Ecotec	1	2,638,554	0.97	0.85	9.02	89.16	9.73	0.94	90.27	99.06	90.13	53.38
	2	2,639,159	0.98	0.84	9.14	89.03	9.71	0.94	90.29	99.06	90.02	53.89
	4	2,639,928	0.99	0.83	9.35	88.82	9.59	0.93	90.41	99.07	89.82	54.31
Project Canary	1	1,354,559	10.15	1.55	0.39	87.91	96.28	1.73	3.72	98.27	98.06	86.79
	2	1,354,747	10.29	1.42	0.41	87.89	96.21	1.59	3.79	98.41	98.18	87.87
	4	1,355,140	10.47	1.26	0.43	87.84	96.05	1.41	3.95	98.59	98.31	89.27
Qube	1	3,146,525	5.90	0.72	5.32	88.07	52.6	0.81	47.4	99.19	93.97	89.19
	2	3,147,247	5.98	0.64	5.40	87.97	52.57	0.73	47.43	99.27	93.96	90.29
	4	3,148,424	6.10	0.55	5.51	87.84	52.55	0.62	47.45	99.38	93.94	91.74
Sensirion	1	3,738,264	8.81	2.57	0.98	87.65	90.01	2.84	9.99	97.16	96.46	77.45
	2	3,738,986	8.92	2.46	1.02	87.60	89.77	2.74	10.23	97.26	96.52	78.36
	4	3,740,124	9.06	2.34	1.08	87.52	89.38	2.6	10.62	97.4	96.59	79.5
SOOFIE	1	2,528,154	7.12	8.06	1.15	83.68	86.13	8.78	13.87	91.22	90.8	46.92
	2	2,528,490	7.23	7.96	1.16	83.66	86.21	8.69	13.79	91.31	90.88	47.6
	4	2,529,363	7.40	7.82	1.17	83.61	86.29	8.55	13.71	91.45	91.01	48.63

2.2 Supplementary quantification results

This section provides the specific steps for generating linear regression plots and evaluating uncertainty for datasets. Quantification results for each team are shown below.

2.2.1 Quantification calculation

The y-intercept in the regression is set to zero, represented by Eq. (1):

$$y = mx \tag{3}$$

Here, m is the slope, x denotes the mean metered emission rate, and y is the central emission estimate from the teams.

The daily average emission rate is derived by setting start and end times for each test date, incorporating valid test intervals and excluding specific internal periods. The mean release rate over the test period, including non-emission times, is then calculated.

The values of R^2 are given in an uncentered manner, following standards for regressions without a y-intercept. Each team's estimate is considered as an independent observation, ensuring a robust regression.

2.2.2 *Quantification plots of individual teams - both stacks*

Four teams participated in quantification testing under both stacks. Project Canary participated exclusively in the short-stack quantification testing. The average reported release rate by each team and the relative average emission released by Stanford is shown in table 19. On average, all participating teams have underestimated emissions by 74.6%.

Table 19: Release rates of daily average quantification estimates

Team	**Mean reported release rate (kg/hr)**	**Mean true release rate (kg/hr)**	**Estimation error compared to Stanford release rate (%)**
Canary	9.97	186.81	-94.67%
Oiler	16.99	227.47	-92.53%
Qube	11.00	173.17	-93.65%
Sensirion	41.85	222.08	-81.14%
SOOFIE	175.11	194.29	-9.87%

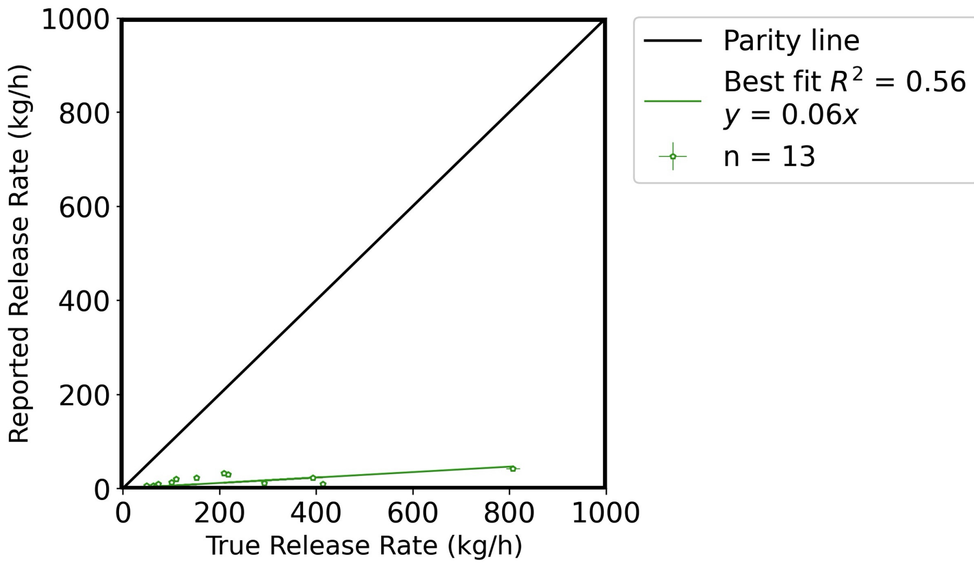

Fig 14: Quantification accuracy for Oiler. The x-axis represents the metered release rate, with error bars indicating the 95% confidence interval (CI). A black parity line, representing the x=y relationship, is drawn on the plot for reference.

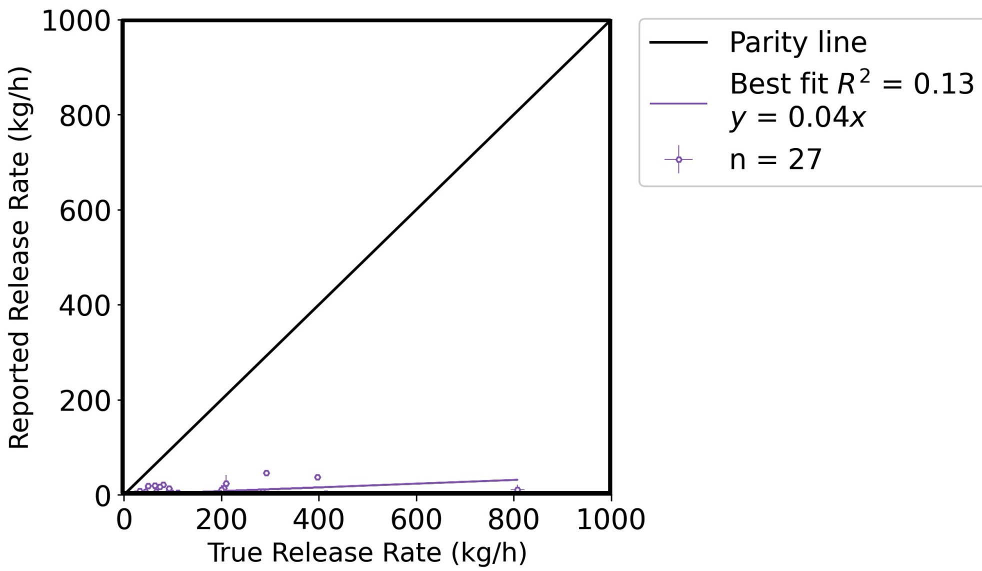

Fig 15: Quantification accuracy for Qube Technology. The x-axis represents the metered release rate, with error bars indicating the 95% confidence interval (CI). A black parity line, representing the x=y relationship, is drawn on the plot for reference.

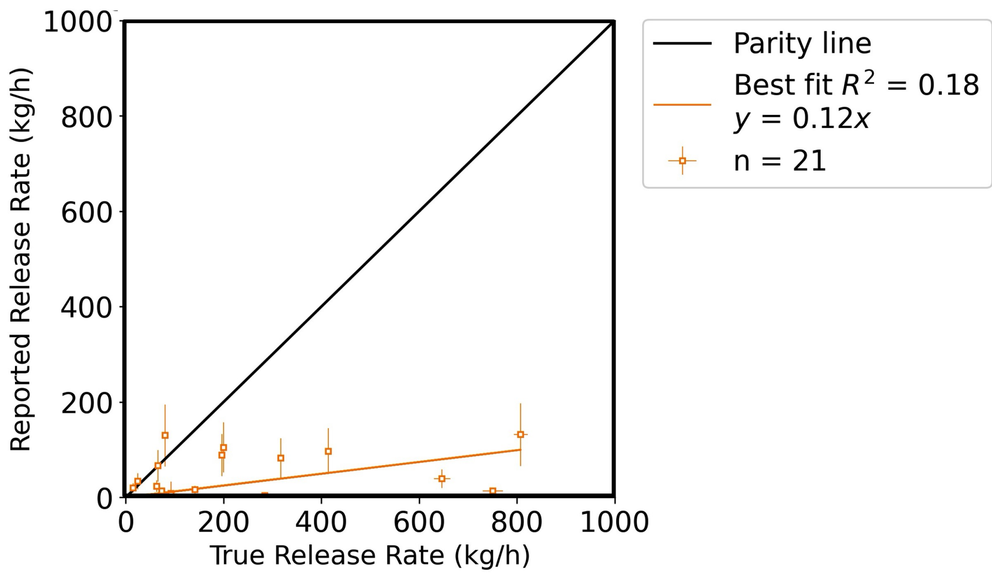

Fig 16: Quantification accuracy for Sensirion. The x-axis represents the metered release rate, with error bars indicating the 95% confidence interval (CI). A black parity line, representing the x=y relationship, is drawn on the plot for reference.

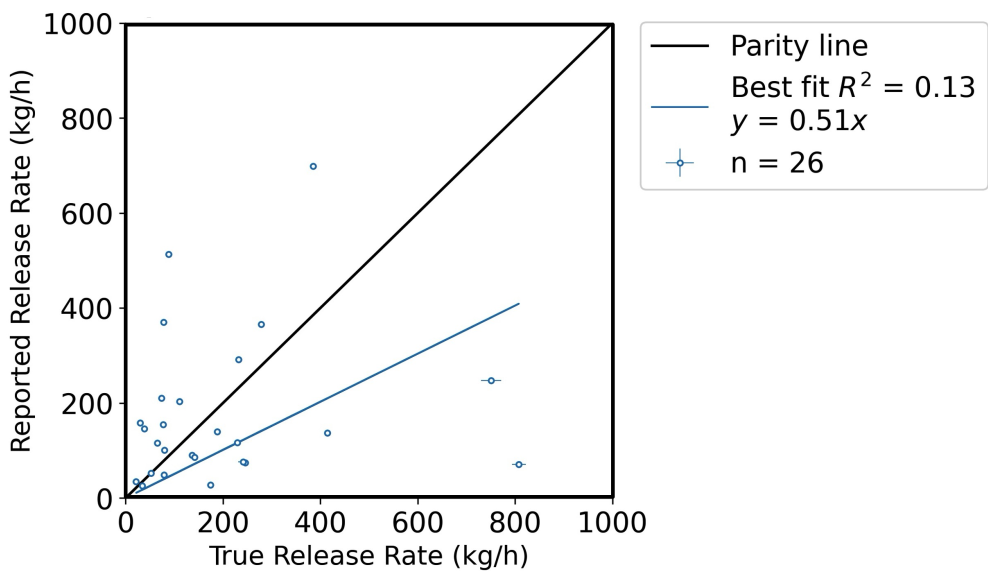

Fig 17: Quantification accuracy for SOOFIE. The x-axis represents the metered release rate, with error bars indicating the 95% confidence interval (CI). A black parity line, representing the x=y relationship, is drawn on the plot for reference.

2.2.3 *Quantification plots of individual teams - short stack*

Project Canary participated exclusively in the short-stack quantification testing. The figures presented below illustrate the quantification performance of four teams during the short stack height period. The Oiler was involved from 10/10/2023 to 11/03/2023. During this period, they missed the significant release phase associated with the short stack height, resulting in insufficient data for generating a quantification plot.

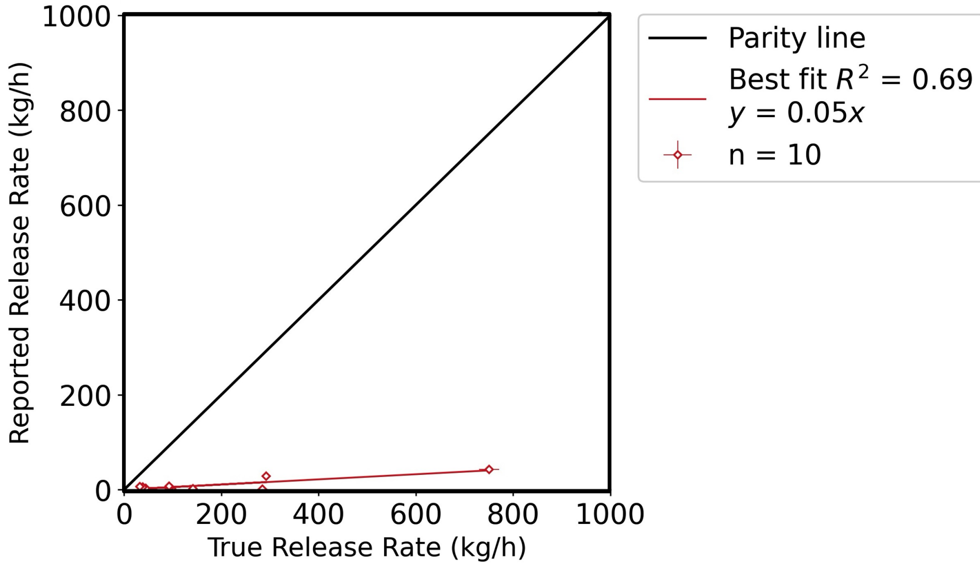

Fig 18: Quantification accuracy for Project Canary. The company is quantified during short stack heights only. The x-axis represents the metered release rate, with error bars indicating the 95% confidence interval (CI). A black parity line, representing the x=y relationship, is drawn on the plot for reference.

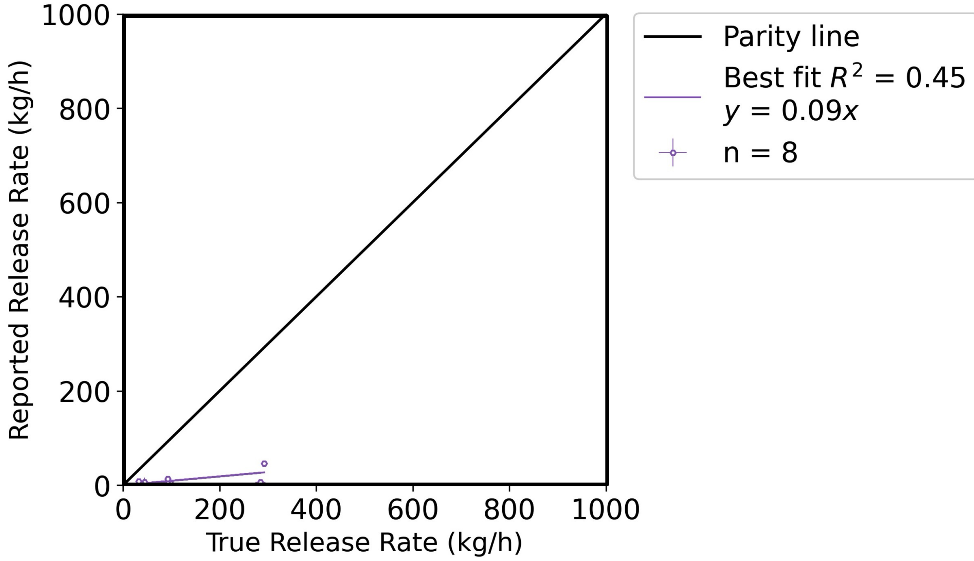

Fig 19: Quantification accuracy for Qube. The x-axis represents the metered release rate, with error bars indicating the 95% confidence interval (CI). A black parity line, representing the x=y relationship, is drawn on the plot for reference.

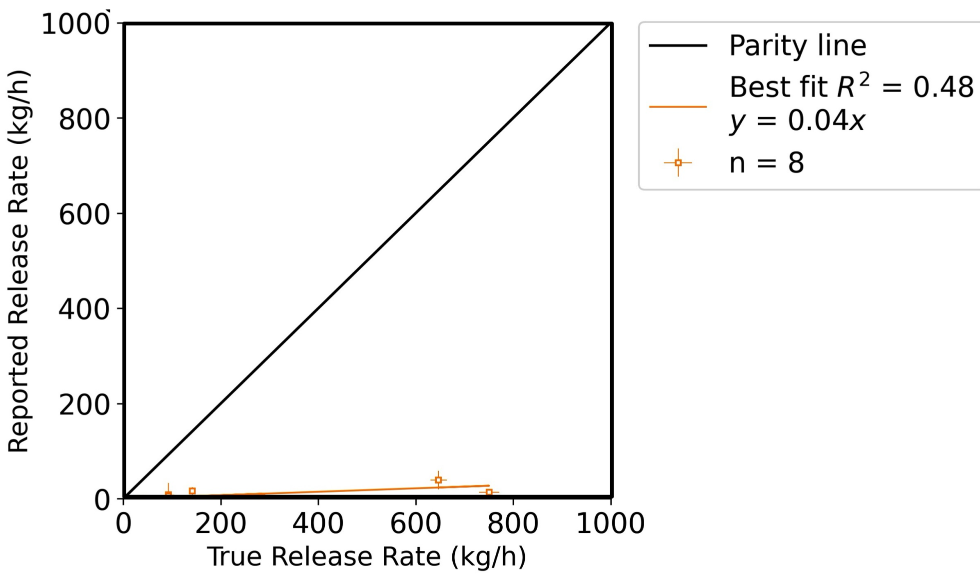

Fig 20: Quantification accuracy for Sensirion. The x-axis represents the metered release rate, with error bars indicating the 95% confidence interval (CI). A black parity line, representing the x=y relationship, is drawn on the plot for reference.

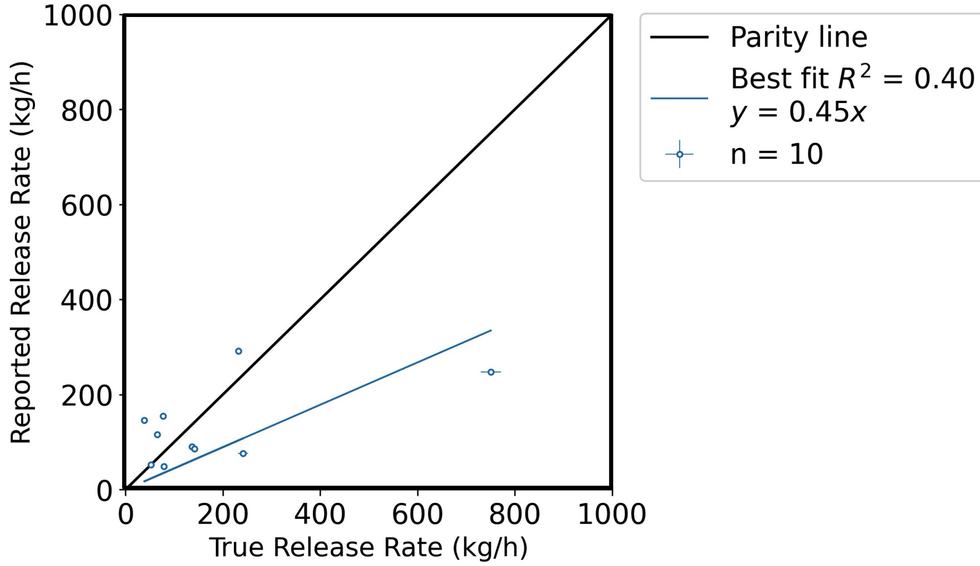

Fig 21: Quantification accuracy for SOOFIE. The x-axis represents the metered release rate, with error bars indicating the 95% confidence interval (CI). A black parity line, representing the x=y relationship, is drawn on the plot for reference.

2.2.4 Quantification plots of individual teams - evaluated on team reported events

Figure 22 illustrates the percentage of quantification error for each team in relation to various methane release rates. This calculation provides a relative measure of each team's accuracy in quantifying methane emissions, where a positive value indicates an overestimation, a negative value is an underestimation, and a value close to zero represents a highly accurate quantification. These insights are crucial for assessing the precision of different continuous monitoring technologies and their potential for application in emission regulation compliance. Figure 23 presents the results of our evaluation of continuous monitoring systems based on their quantification of reported emission events. This approach offers higher time resolution estimates compared to the daily average emission rate results discussed in the main paper. However, it's important to note that these estimates tend to be noisy and more challenging to interpret. On average, all participating teams have underestimated emissions by 47.1%. The average reported release rate by each team and the relative average emission released by Stanford are shown in Table 20. Project Canary participated exclusively in the short-stack quantification testing. The result of team's general underestimation aligns with the approach using the daily average release rate.

Table 20: Release rates of team-reported average quantification estimates

Team	**Average report release rate (kg/hr)**	**Average Stanford release rate (kg/hr)**	**Estimation error compared to Stanford release rate (%)**
Project Canary	9.97	186.81	-94.67%
Qube	13.56	203.64	-93.33%
Sensirion	45.39	219.57	-79.34%
Oiler	26.71	343.180	-92.22%
SOOFIE	193.66	155.70	+24.38%

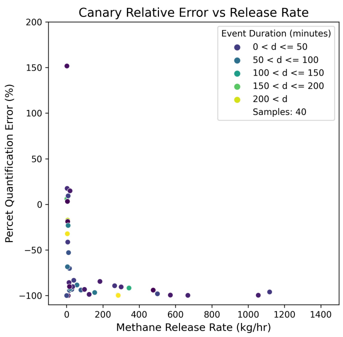

(a) Project Canary

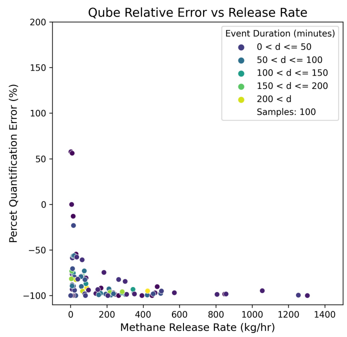

(b) Qube

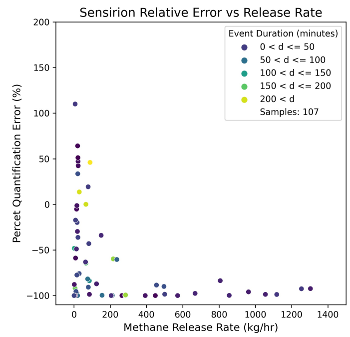

(c) Sensirion

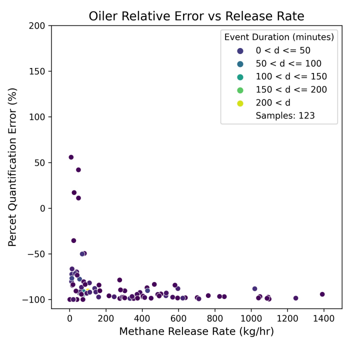

(d) Oiler

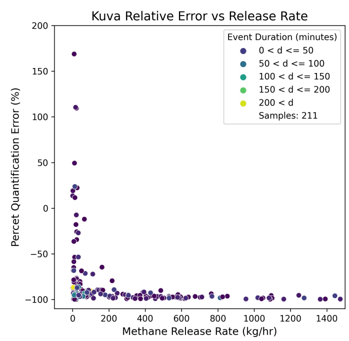

(e) Kuva

Fig 22: Relative error of quantification vs. release rate. These sub-graphs plot the relative error in quantification against the methane release rate (in kg/hr) for each respective technology. X-axis represents the rate at which methane was released during the experiment, measured in kilograms per hour (kg/hr). Y-axis Indicates the error in the quantification of methane as a percentage. Positive values represent an overestimation, while negative values represent an underestimation of the actual release rate. Each point represents an individual measurement event, colored according to the duration of the event as indicated by the legend. Different colors correspond to event durations, ranging from under 50 minutes to over 200 minutes. The number below each sub-graph denotes the total number of samples or measurement events included for that sensor technology. From these sub-graphs, one can interpret how accurately each sensor technology quantified the methane release at varying rates and event durations. A high density of points near the 0% line would suggest accurate quantification, while points farther away indicate greater errors in quantification. This visualization helps in understanding each technology's precision and reliability in methane detection and quantification across a range of release scenarios.

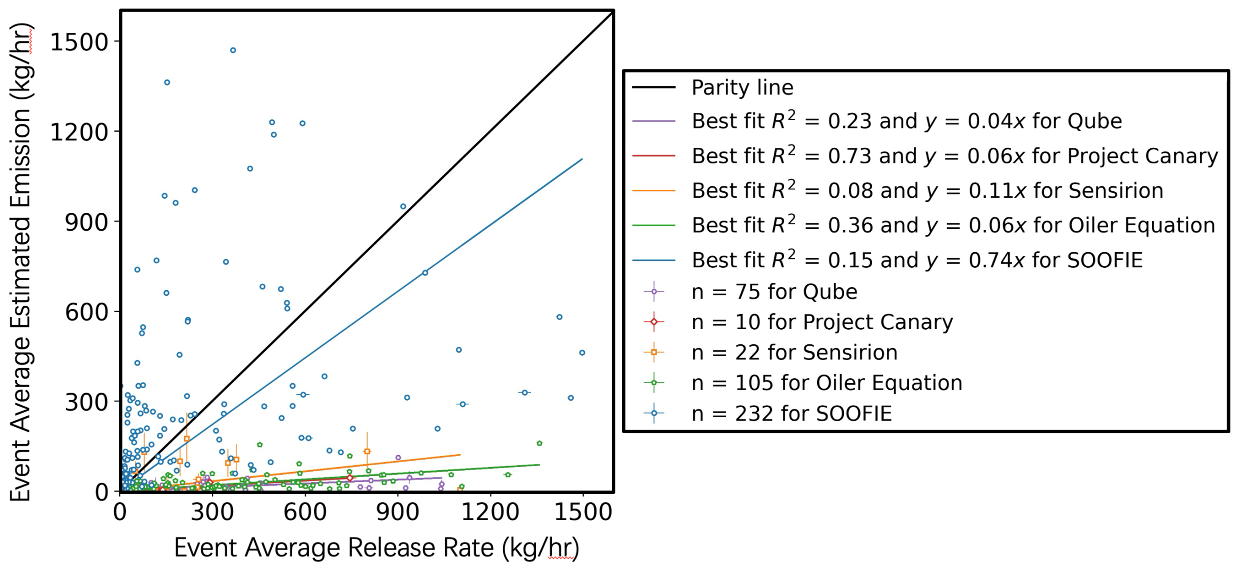

Fig 23: Event-based average quantification plot for systems: The x-axis represents the daily average methane release rate as recorded by Stanford, with error bars indicating the 95% confidence interval (CI). These CI bars might be barely visible due to their small size. The y-axis shows the daily average release rate reported by the continuous monitoring solutions. Here, error bars represent the reported 95% CI uncertainty for all participants, except for SOOFIE who did not report this uncertainty. The black line indicating x=y represents parity between the recorded and reported rates. Data from each system or team is color-coded for easy differentiation. This graph underscores that while higher time resolution quantification is achieved, these estimates are generally noisy and complex to interpret.

2.2.5 Error bars of true release for quantification results

To determine the error bars associated with the true release, we rely on a mathematical approach based on uncertainties tied to gas measurements and methane mole fraction.[15] The relative variability for the gas flow rate is determined by comparing the standard deviation of the meter's readings to the average flow rate over the day. Similarly, the relative variability for the methane fraction is ascertained by comparing its standard deviation to its mean value over the day. Once these relative variabilities are obtained, we derive the combined uncertainty for the methane flow rate by mathematically amalgamating these two variabilities using the quadrature sum method. This method provides insight into the fluctuations associated with both the flow rate and the methane fraction, ensuring the reliability of our quantification.

The calculations are as follows:

$$X = \text{Average of observed values} = \frac{1}{N}\sum_i x_i \tag{4}$$

$$U = \text{Upper bound of the confidence interval} = X + \frac{1}{N}\sum_i (1.96 \times \sigma_i x_i) \tag{5}$$

$$L = \text{Lower bound of the confidence interval} = X - \frac{1}{N}\sum_i (1.96 \times \sigma_i x_i) \tag{6}$$

Table 21: Daily average uncertainty rate for quantification analysis

Team	Data Type	Samples	Range	Mean ± Std	Min emission	Max emission
Project Canary	Stanford Releases	10	[0.049, 20.776]	[0, 10.969]	[32.065, 32.164]	[729.778, 771.329]
	Team Reported Emissions	10	[0, 0]	[0, 0]	[1.142, 1.142]	[42.192, 42.192]
Oiler	Stanford Releases	13	[0.206, 14.078]	[0, 7.000]	[49.241, 50.143]	[793.581, 821.737]
	Team Reported Emissions	13	[0.046, 0.770]	[0.071, 0.532]	[2.658, 2.750]	[40.800, 42.339]
Qube	Stanford Releases	27	[0.049, 14.078]	[0, 6.208]	[24.574, 24.687]	[793.581, 821.737]
	Team Reported Emissions	27	[0, 17.964]	[0, 6.664]	[0.702, 0.971]	[43.556, 47.919]
Sensirion	Stanford Releases	21	[0.056, 20.776]	[0, 10.527]	[14.810, 15.353]	[793.581, 821.737]
	Team Reported Emissions	21	[0.150, 65.800]	[0, 44.222]	[0.150, 0.450]	[65.800, 197.400]
SOOFIE	Stanford Releases	26	[0.049, 20.776]	[0, 8.224]	[21.341, 21.883]	[793.581, 821.737]
	Team Reported Emissions	26	[0, 0]	[0, 0]	[25.531, 25.531]	[698.471, 698.471]

Where:

- X is the average of the observed values.
- U and L represent the upper and lower bounds of the 95% confidence interval, respectively.
- σ_i is the standard deviation for the i^{th} observation, determined by:

$$\sigma = x_i \sqrt{\left(\frac{\sigma_{\text{gas\_flow}}}{x_{\text{gas\_flow}}}\right)^2 + \left(\frac{\sigma_{\text{fraction\_methane}}}{x_{\text{fraction\_methane}}}\right)^2} \tag{7}$$

Here, $\sigma_{\text{gas\_flow}}$ and $\sigma_{\text{fraction\_methane}}$ are the uncertainties in the gas flow rate and methane fraction, respectively. $x_{\text{gas\_flow}}$ and $x_{\text{fraction\_methane}}$ are the corresponding observed values.

2.2.6 Error bars of team reported release

Error bars for reported releases depict the variability in the data. The methodology to compute these is given by the standard deviation estimate formula:

$$\hat{\sigma} = \frac{1}{N} \sum_i (\hat{x}_i - x_i) \times \lambda_i \tag{8}$$

In this equation:

- $\hat{\sigma}$ is the estimated standard deviation.
- N is the total number of data points.
- $\hat{x}_i$ and x_i are the estimated and actual values of the i^{th} observation, respectively.
- λ_i is the weighting factor for the i^{th} observation.

The term $(\hat{x}_i - x_i)$ calculates the discrepancy between estimated and actual values. This is then multiplied by the weighting factor, λ_i, and summed across all observations. The result, divided by N, gives the estimated standard deviation used for the error bars.

2.3 Exhibits

2.3.1 Visits and changes to the equipment setup

During the experiment, Technicians from continuous monitoring teams that were allowed routine supervised site visits to check equipment functionality and make necessary adjustments.

2.3.2 Project Canary short stack height proposal

Proposal for Stanford Controlled Release Testing with Project Canary

Stanford University will conduct controlled release trials to evaluate the performance of methane detection and/or quantification systems in Fall 2022. We will conduct releases ranging from less than 10 kgCH4/hr to over 1,500 kgCH4/hr, using stacks with different heights. Large emissions will be released from a taller stack (~5-10 m tall). To ensure safety of all field researchers and personnel, release from a shorter stack (~1-2 m tall) will be limited to lower release volumes.

Project Canary will participate with their continuous monitoring system and report methane fluxes to Stanford for releases from the lower-height methane stack. As a fully blind participant, Project Canary will set up their Canary X methane detection system onsite for testing. As determined by Project Canary, the Canary may be set up for up to the entire 2-month duration of the campaign. Using data collected during this period, Project Canary will estimate methane fluxes from the release point.

After the test period is complete, Project Canary will report detections and flux estimates for releases from the short-release stack (as well as localization information if desired). Stanford will report to Project Canary the time periods in which methane was released from the taller stack, and Project Canary may remove these periods from all analysis reported to Stanford. Otherwise, Project Canary will participate in the unblinding process (described below) followed by all other teams. Project Canary will agree to keep information regarding timings of release from different stack heights as confidential until full release data are unblinded for all participating teams.

The unblinding process will follow approaches previously developed by Stanford, subject to minor modifications. Briefly, teams will first report their fully blinded results. Next, Stanford will release 10 meter wind data collected onsite during the tests, and allow teams to re-analyze and report modified values. In the final stage of unblinding, Stanford will release a subset of data collected for teams to use as a training dataset. Teams will have a final opportunity to make modifications to their analysis and submit adjusted results.

Fig 24: Project Canary short stack height proposal to Stanford research team. This is the original proposal received before the control release test on Oct 10, 2022.

References

1 C. Bell and D. Zimmerle, *METEC controlled test protocol: continuous monitoring emission detection and quantification*. PhD thesis, Colorado State University. Libraries.

2 S. Henry and D. Zimmerle, "Advancing development of emissions detection (aded)," Project Report FE0031873, Colorado State University, Fort Collins, CO 80523 (2023).

3 Andium, "Andium: Homepage," (2023). Accessed: 2023-10-15.

4 P. Canary, "Project canary: Homepage," (2023). Accessed: 2023-10-15.

5 Ecotec, "Ecotec: Homepage," (2023). Accessed: 2023-10-15.

6 K. Systems, "Kuva systems: Homepage," (2023). Accessed: 2023-10-15.

7 O. Equation, "Oil equation: Homepage," (2023). Accessed: 2023-10-15.

8 Q. IoT, "Qube iot: Homepage," (2023). Accessed: 2023-10-15.

9 S. Connected, "Emissions monitoring," (2023). Accessed: 2023-10-15.

10 ChampionX, "Continuous emissions monitoring - soofie," (2023). Accessed: 2023-10-15.

11 B. Hughes, "Lumen terrain case study," (2021). Accessed: 2024-01-15.

12 Honeywell, "Gas cloud imaging." Accessed: 2024-01-15.

13 P. Photonics, "Providence photonics: Shedding light on the invisible," (2024). Accessed: 2024-01-15.

14 C. AI, "Cleanconnect.ai," (2024). Accessed: 2024-01-15.

15 S. H. El Abbadi, Z. Chen, P. M. Burdeau, *et al.*, "Comprehensive evaluation of aircraft-based methane sensing for greenhouse gas mitigation," (2023).